# N O T I C E

THIS DOCUMENT HAS BEEN REPRODUCED FROM MICROFICHE. ALTHOUGH IT IS RECOGNIZED THAT CERTAIN PORTIONS ARE ILLEGIBLE, IT IS BEING RELEASED IN THE INTEREST OF MAKING AVAILABLE AS MUCH INFORMATION AS POSSIBLE

NASA Contractor Report 165246

# ON VARIABLE HYDROSTATIC TRANSMISSION
# FOR ROAD VEHICLES, POWERED BY SUPPLY
# OF FLUID AT CONSTANT PRESSURE

Mart Mägi
Solvo AB
31 Hammarliden
S - 412 62 Gothenburg, Sweden

and

Are Freivald
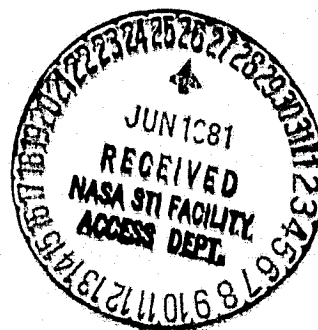Volvo Flygmotor AB
S - 461 01 Trollhätten, Sweden

and

Ingvar Andersson and Ulf Ericsson
Solvo AB
31 Hammarliden
S - 412 62 Gothenburg, Sweden

May 1981

# CONTENTS <span style="float:right">Page</span>

# LIST OF ILLUSTRATIONS

## PREFACE

This work has been performed as part of the NASA LERC PROJECT under Contract NASW-3299. It has been carried out as a joint effort by Volvo Flygmotor AB, Trollhättan, and Tekniska Konsultbyrån SOLVO AB, Gothenburg, Sweden.

Volvo Flygmotor AB has served as the main contractor, performing the experimental part of the work and supporting the analytical part with its know-how and design experience.

The analysis has been carried out on a subcontract basis by Tekniska Konsultbyrån SOLVO AB, a group of consultants consisting of Members of the Staff of the Dept. of Mechanical Engineering, Chalmers University of Technology, Gothenburg, Sweden.

This report includes a consolidation of five separate reports on Tasks I through V,

TASK I:     Screening of Candidate Hydraulic Drive Systems

TASK II:    Testing of Hydraulic Motors and Pumps at Low RPM, Low Volume Conditions

TASK III:   System Performance Optimization with Constant Differential Hydraulic Pressure

TASK IV:    Quantitative Behavior and Losses of Volvo Flygmotor Motors/Pumps

TASK V:     Back Pressure Performance Evaluation at Constant Differential Pressure

SI units have been used throughout this report, although the primary project specification was given in imperial units.

The few references used are identified by notes on the pages where they appear.

The responsibilities of the four co-authors have been as follows:

Mr ARE FREIVALD, Volvo Flygmotor AB, has served as project coordinator.

Dr MART MÄGI, SOLVO AB, has served as scientific and technical director of the project and has written the final report

Dr INGVAR ANDERSSON, SOLVO AB, has been responsible for the lay-out of the computer program and has written all subroutines, except those on the modeling of components and the optimization

Dr ULF ERICSSON, SOLVO AB, has programmed the modeling of components, including the fitting of loss coefficient to experimental data.

September 1980

Mart Mägi                                    Åre Freivald
Gothenburg                                   Trollhättan

Ingvar Andersson                             Ulf Ericsson
Gothenburg                                   Gothenburg

## ACKNOWLEDGEMENTS

## NOTATION

| | | | |
|---|---|---|---|
| m | [kg] | = | vehicle weight (mass) |
| p | $[N/m^2]$ | = | pressure |
| $\Delta p$ | $[N/m^2]$ | = | differential pressure |
| q | $[m^3/s]$ | = | flow rate |
| $\Delta q$ | $[m^3/s]$ | = | flow loss, leakage |
| v | [m/s] | = | vehicle speed |
| A | $[m^2]$ | = | piston area |
| C | [-] | = | loss coefficient, clutch |
| D | $[m^3/rev]$ | = | displacement per revolution |
| D' | $[m^3/rad]$ | = | displacement per radian |
| E | [Nm] | = | energy |
| F | [N] | = | force (driving) |
| L | [m] | = | length (of driving cycle) |
| P | [W] | = | power |
| $\Delta P$ | [W] | = | power loss |
| R | [-] | = | transmission ratio |
| R' | [1/m] | = | transmission ratio of final gear |
| T | [Nm] | = | torque |
| $\Delta T$ | [Nm] | = | torque loss |
| Vo | $[m^3]$ | = | package volume |
| We | [kg] | = | package weight (mass) |
| $\alpha$ | [°] | = | yoke or swash plate angle |
| $\varepsilon$ | [-] | = | fraction of maximum displacement |
| $\eta$ | [-] | = | efficiency |
| $\theta$ | [-] | = | size ratio |
| $\mu$ | $[Ns/m^2]$ | = | absolute viscosity |
| $\rho$ | $[kg/m^3]$ | = | density |
| $\omega$ | [rad/s] | = | angular velocity |

## Subscripts (selected)

| | | |
|---|---|---|
| vol | = | volumetric, see efficiency of speed transmission |
| mech | = | mechanical, see efficiency of speed transmission |
| tot | = | total, see efficiency of speed transmission power |
| var | = | variable, see displacement |
| fract | = | fractional, see displacement |
| max | = | see displacement and force |
| conn | = | connect, see ratio of connecting drive |
| low | = | low gear, see ratio of planetary drive |
| theor | = | theoretical, losses neglected |
| equ | = | equivalent, see pressure |
| back | = | see pressure |

# 1. DESIGN SPECIFICATIONS

The scope of Contract NASW-3299, within the NASA LERC PROJECT, concerns the principal development, evaluation, and optimization of a power transmission system of a road vehicle, where the prime mover (such as a free-piston Stirling engine) produces hydraulic energy, available at constant pressure and with no short-term limitations on flow rate. The power transmission system is to be based upon the Volvo Flygmotor V-20 type variable displacement motor/pump as the principal unit.

According to the contract, the transmission system was to be designed and sized to meet the performance criteria specified below, at the same time minimizing:
- size
- weight
- complexity

and exhibiting optimum efficiency when cruising at constant speed within the range of 6.7 through 22.4 m/s (15 through 50 mph).

During the course of the work the efficiency criteria were re-formulated to the following, more precise, terms:

the transmission system should exhibit, when optimized, the lowest possible energy consumption when completing an EPA Urban Driving Cycle.

The steady-state speed road load was to be based on the following prescribed expression:

$$P = 228.6 * v + 1.06 * v^2 + 0.5775 * v^3 \qquad (1)$$

where P = power on driving wheels in W

$v$ = vehicle speed in m/s

The weight m of the vehicle was prescribed to be:

$$m = 1542 \text{ kg (3400 pounds)} \qquad (2)$$

The special performance criteria to be met were:

- The minimum distance to be covered in 10 s from a standing start is 134 m (440 feet)

- The maximum time to reach a speed of 26.8 m/s (60 mph) from a standing start is 15 s

No special gradability criteria were prescribed.

## 2. REQUIRED DRIVING FORCE

The most important quantity in the design and analysis
of the propulsion systems of road vehicles is the total
driving (or braking) force $F$ acting on the periphery of
the driving wheels.

The instantaneous value of F defines:

- either the cruising speed $v$ (when F is in equilibrium
  with the road load and with the component of the vehicle
  weight, when grading)

- or the acceleration/deceleration (when F exceeds/falls
  below the road load)

The vehicle speed $v$ is thus controlled by the driving force
F, and it is appropriate to discuss the design criteria as
well as the transmission performance in F vs. $v$ diagrams
(see Fig. 1). Note that such diagrams also contain infor-
mation on the output power P (W), because

$$P = F*v \tag{3}$$

The F vs. $v$ diagram will be used from here on in this report
to discuss design criteria and transmission performance.

Cruising at steady-state speed requires the following
driving force (cf. Eq. 1):

$$F = 228.6 + 1.06*v + 0.5775*v^2 \tag{4}$$

which may be interpreted as

- 1.5 % rolling resistance

- a frontal area of 3.2 m$^2$ at a 0.30 aerodynamic drag
  coefficient
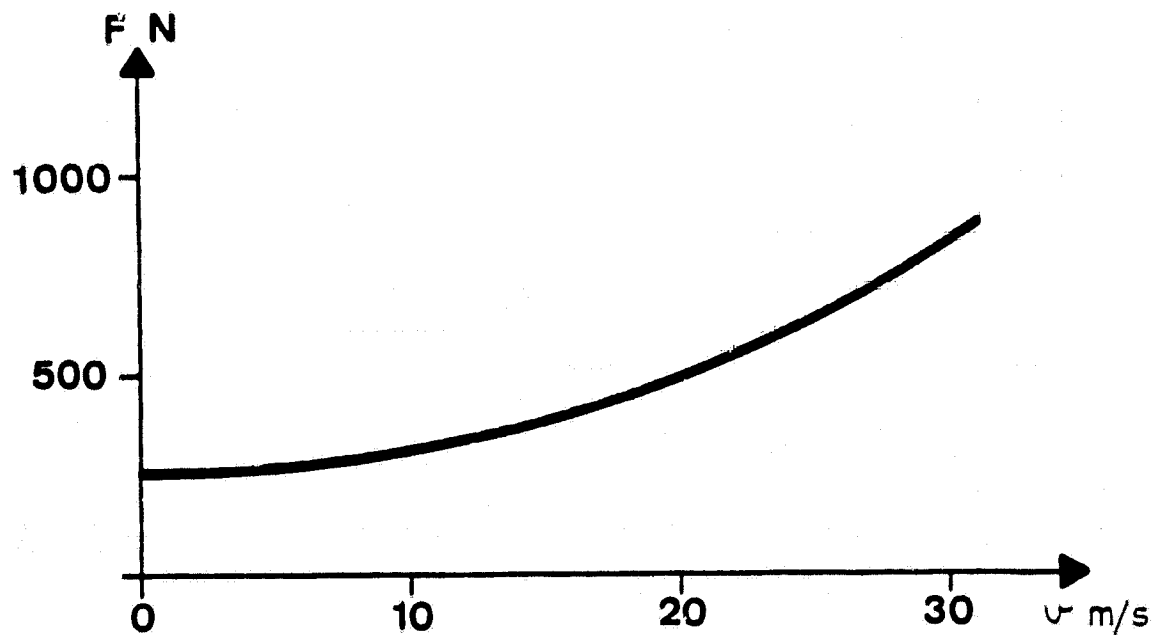
Fig. 1. Road load F vs. cruising speed ʋ

The acceleration criteria may be met by various F vs. ʋ
configurations. Conventional automobiles with a manual
four-speed transmission produce high driving forces in
the low-speed regime (limited by wheel spin) and low
driving forces in the high-speed regime (limited by engine
power) as indicated in
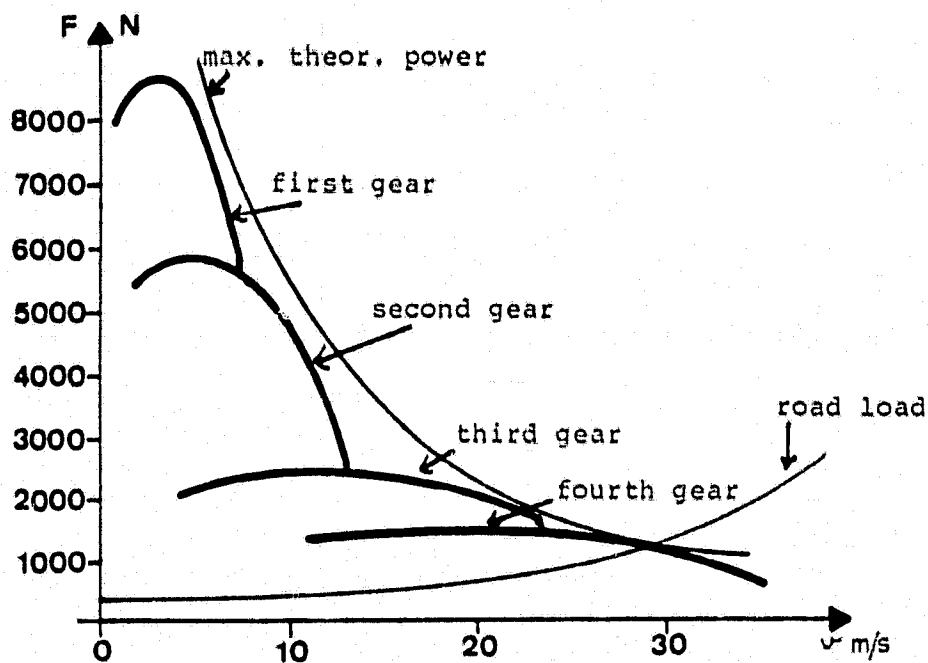


Fig. 2. Road load and available driving force when a manual
four-speed transmission is used

In the present design situation it is possible to choose
an alternative approach. The same constant maximum driving
force may be utilized over the whole speed regime, as
there are no short-term power-supply limitations. The
maximum driving force is thereby reduced, resulting in
reduced weight and size of the final drive.

If the rise time for the driving force and time lost
when shifting gears are neglected, a net acceleration force
may be calculated to meet the performance criteria:
- acceleration from standing start to 134 m in 10 s
  requires $F_{acc}=4140$ N, and the corresponding maximum
  driving force must also include the road load, thus
  $F_{max}=4600$ N (approx)

- acceleration from standing start to 26.8 m/s in 15 s
  requires $F_{acc}=2760$ N, and with the road load added,
  $F_{max}=3250$ N (approx)

Driving force requirements, established by the EPA Urban
Driving Cycle, are calculated as follows:

The driving cycle is defined over a period of 1372 s,
and the vehicle speed is specified for each second (cf. F 3).
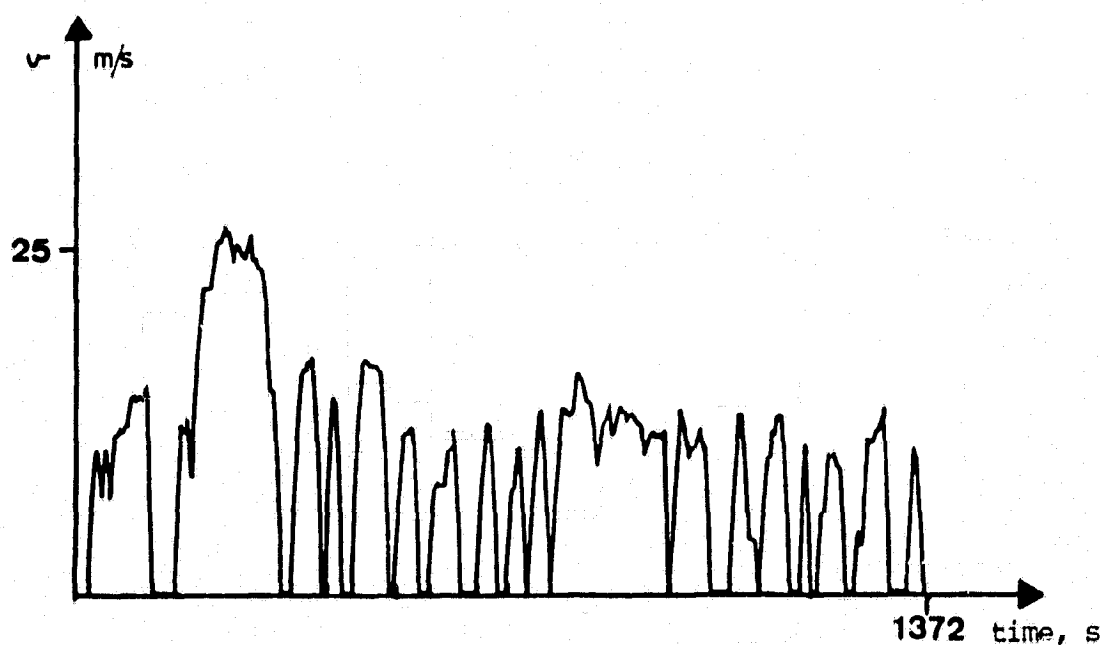


Fig. 3. EPA Urban Driving Cycle

Polynomials of the third power have consecutively been fitted to four adjacent, defined points on the EPA Cycle. Time derivatives of the polynomials yield vehicle accelerations.

Vehicle speed and acceleration have been calculated at time increments of 0.1 s over the driving cycle. The cycle length has been integrated to:

$$L = 11.99 \text{ km} \tag{5}$$

For each time increment the total driving (or braking) force has been calculated as the sum of the road load (from Eq. (4)) and the product of the vehicle mass and acceleration (deceleration). The resulting 13,720 values have been grouped in a driving cycle matrix (F4), where the increments are 0.5 m/s for speed and 50 N for force. About 5000 different combinations of F and $v$ appear, with peak F values at about 2600 N, and peak speeds at 25 m/s. Negative (i.e., braking) forces have been omitted from the matrix.
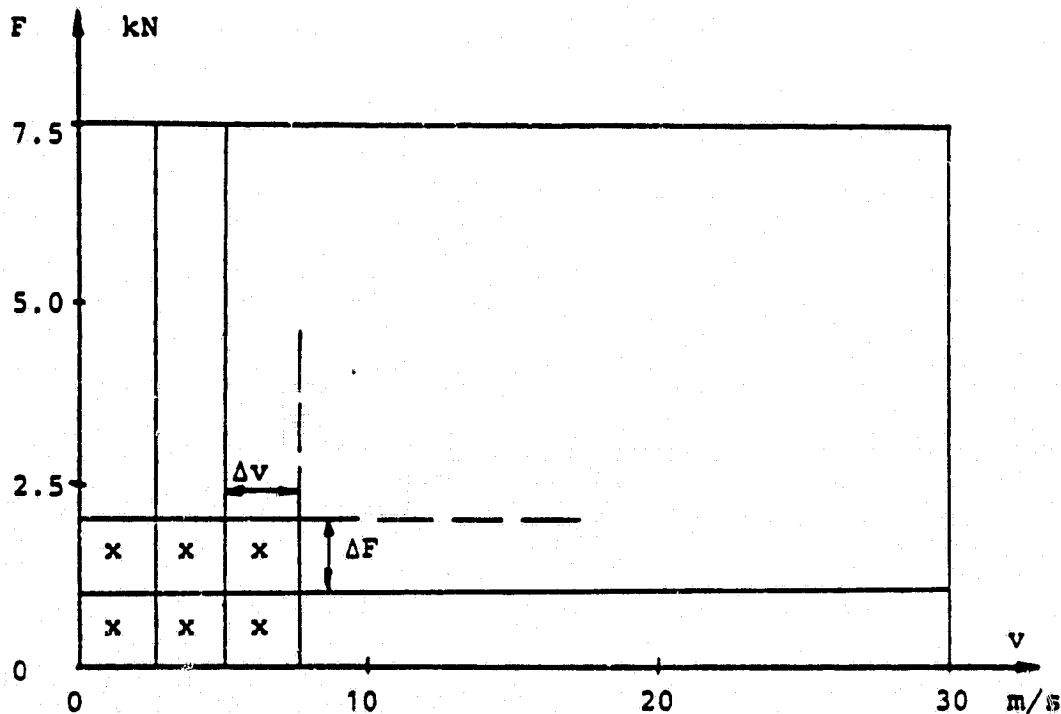


x = duration of requested combination of F and v
$\Delta F$ = force increment, $\Delta v$ = speed increment

Fig. 4. Driving cycle matrix F vs. $v$

Based upon the preceding discussions, the driving force requirements are summarized in F5.
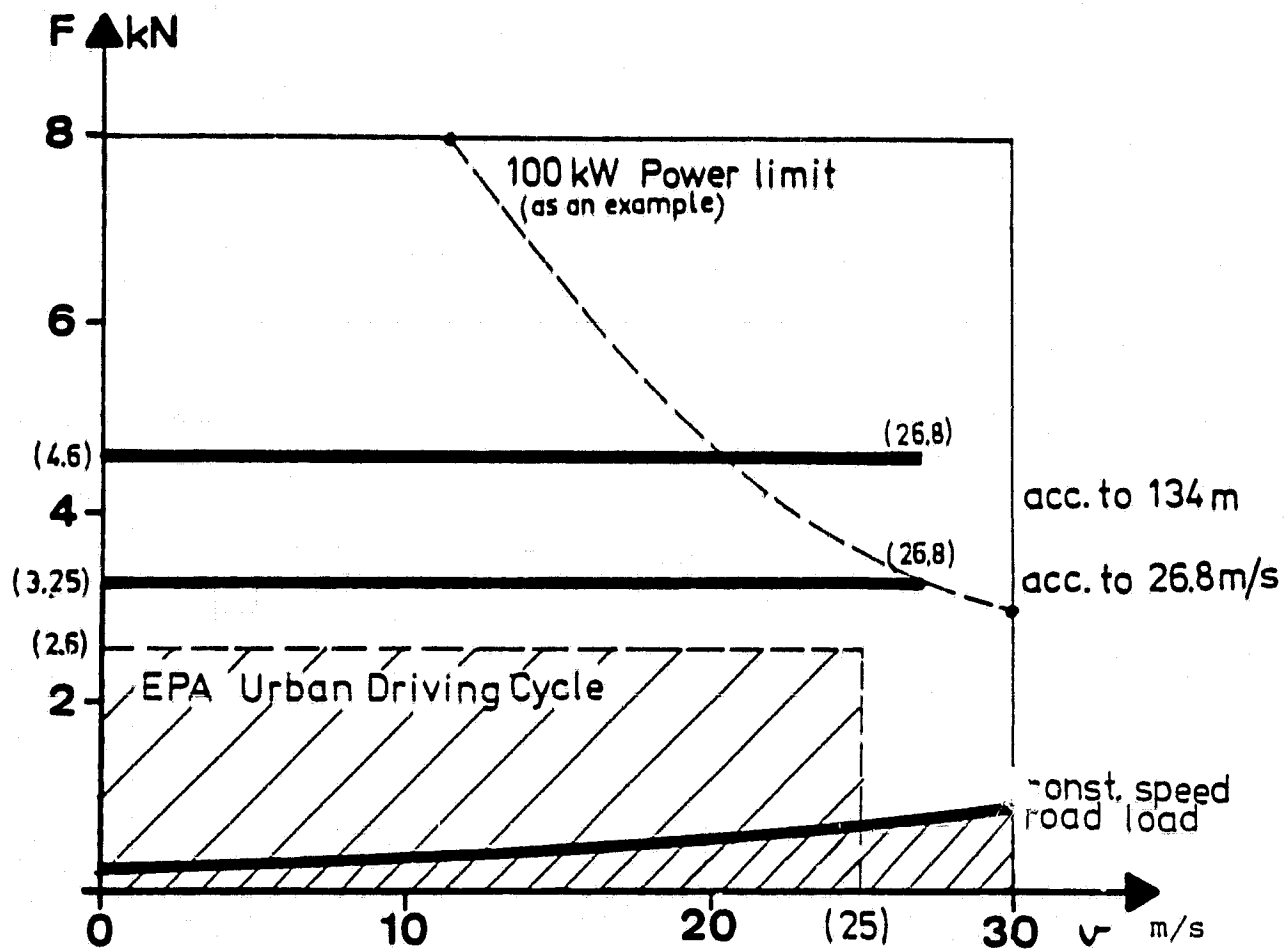


Fig. 5. Driving force requirements

## 3. CHARACTERISTICS OF VARIABLE DISPLACEMENT MOTORS/PUMPS

### General background

Hydrostatic machinery is used either to convert mechanical power into hydrostatic power (pumps) or vice versa (motors).

Hydrostatic power is defined by:

$\Delta p$ = hydrostatic differential pressure in $N/m^2$

$q$ = flow rate in $m^3/s$

$P = \Delta p * q$ = power in W

The theoretical power transmission relationships are easily understood for the linear mode of operation, e.g., for actuators:

equilibrium yields

$$F = \Delta p * A \tag{6}$$

continuity yields

$$q = \sigma * A \tag{7}$$

where A is the actuator area $(m^2)$

Similar relationships hold for transmissions operating in the rotational mode:

equilibrium yields

$$T = \Delta p * D' \tag{8}$$

continuity yields

$$q = \omega * D' \tag{9}$$

where  $T$ = torque in Nm

$\omega$ = rotational speed in rad/s

and  $D'$ = hydraulic displacement in $m^3/rad$

Instead of $D'$, data sheets etc. from manufacturers often give the displacement in another unit, namely:

$D$ = hydraulic displacement in vol/one rev.

The two displacements are interrelated by:

$$D = 2 * \pi * D' \tag{10}$$

The basic relationships, Eqs. (6) through (9), indicate that

load transmission: $F$ or $T \leftrightarrows \Delta p$

and

speed transmission: $\sigma$ or $\omega \leftrightarrows q$

do not mutually influence each other. The transmission ratio is for both cases $D'$ in the rotational mode and $A$ in the linear mode.

There are designs of hydrostatic machinery where a continuous change of the displacement is possible. Such units may thus be considered as Continuously Variable Transmissions, (CVT's).

In the case of variable displacement machines, for each machine exists a maximum displacement $D'_{max}$.

The displacement change could then be expressed by a non-dimensional quantity $\varepsilon$ -displacement fraction - defined as follows:

$$D'_{fract} = \varepsilon * D'_{max} \tag{11}$$

$$|\varepsilon| \leq 1$$

In a formal analysis (where the machine design is adequate)

$$\varepsilon \gtrless 0 \tag{12}$$

could be used, whereby the transition from positive to negative $\varepsilon$ corresponds to a transition from motor to pump operation or vice versa, provided that the hydraulic connection and the direction of $\Delta p$ are unchanged. If not otherwise stated, $\varepsilon > 0$ means motor operation and $\varepsilon < 0$ means pump operation.

In real transmissions the power conversion is influenced by unavoidable losses. The theoretical, no loss reationships, Eqs. (8) and (9), are then modified to:

motor operation:

$$T = \eta_{mech} * D' * \Delta p \tag{13}$$

$$\omega = \eta_{vol} * q/D' \tag{14}$$

pump operation:

$$\Delta p = \eta_{mech} * T/D' \tag{15}$$

$$q = n_{vol} * D' * \omega \tag{16}$$

$\eta_{mech}$ and $\eta_{vol}$ denote mechanical and volumetric efficiencies, respectively. By definition the efficiencies are limited to the interval:

$$0 \leq (\eta_{mech} \text{ and } \eta_{vol}) < 1 \qquad (17)$$

Efficiency is normally defined for power transmission, whereby

$$P_{out} = \eta_{tot} {}^* P_{in} \qquad (18)$$

Substitution for the hydraulic and mechanical power yields the same expression for $\eta_{tot}$ at both motor and pump operation:

$$\eta_{tot} = \eta_{vol} {}^* \eta_{mech} \qquad (19)$$

Note that $\eta_{mech}$ and $\eta_{vol}$ are not constants. In most cases, however, they could be described with reasonable accuracy as functions of load, speed, and fractional displacement, or

$$\eta = f(\Delta p, \omega, \varepsilon) \qquad (20)$$

## Volvo Flygmotor motors/pumps

Volvo Flygmotor has produced and is marketing hydrostatic machines since 1970 . The products are all of the axial piston type, a design concept that makes continuous change of displacement possible.

The axial piston machines could be divided into two groups:
- the bent axis-type

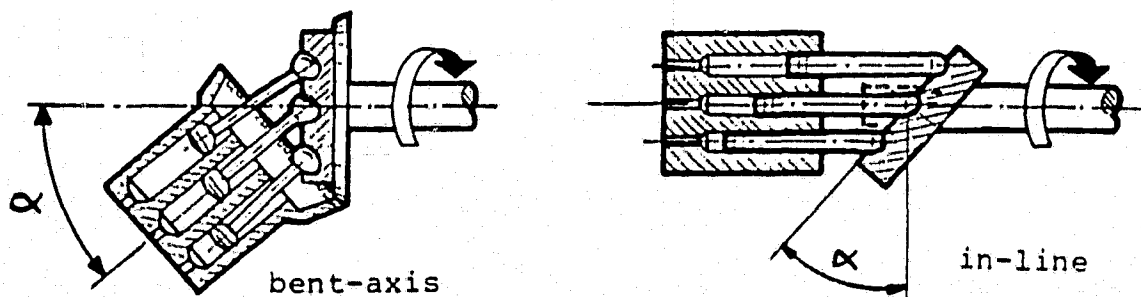- the in-line type (see F6):



Fig. 6. Types of axial piston machines

The product introduced first was the fixed displacement
F-11 series machine. The design concept is of the bent-
axis type, which is made possible by the unique, patented
spherical piston, reducing the piston losses to a minimum.

Before modifying the F-11 series to a variable displacement
version, the V-30 in-line type of variable displacement
machines was introduced. This design cannot take advantage
of the spherical piston.

The third step of development was the V-20 bent-axis type
variable displacement machine, which takes full advantage
of the spherical piston, contributing to the high efficiency
of such machines.

The displacement fraction $\mathcal{E}$ is related to the yoke or swash
plate angle $\alpha$ as follows:

<u>in-line type:</u>

$$\mathcal{E} = \tan \alpha / \tan \alpha_{max} \tag{21}$$

<u>bent-axis type:</u>

$$\mathcal{E} \simeq \sin \alpha / \sin \alpha_{max} \tag{22}$$

Some general characteristics of the efficiencies of Volvo
Flygmotor pumps and motors are:
- At any reasonable fractional displacement $\mathcal{E}$ and rotating
  speed $\omega$ the mechanical efficiency $\eta_{mech}$ decreases to
  zero in the low-pressure regime, (cf. F 7). This is due
  to unavoidable parasitic friction.
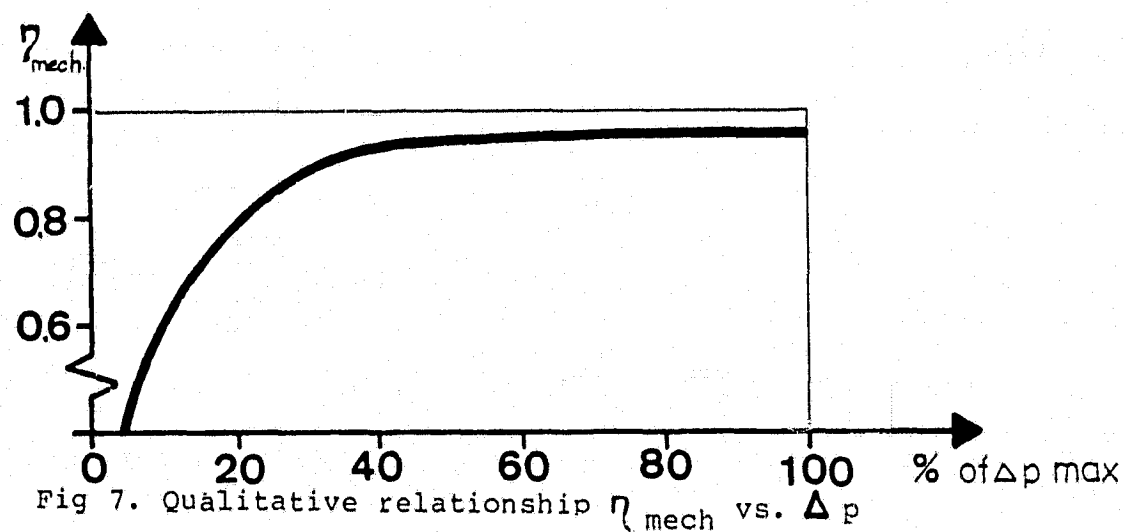


Fig 7. Qualitative relationship $\eta_{mech}$ vs. $\Delta p$

- At any reasonable fractional displacement $\varepsilon$ and differential
  pressure $\Delta p$, the volumetric efficiency $\eta_{vol}$ decreases
  to zero in the low-speed regime (cf. F 8), due to
  unavoidable clearance leakage.
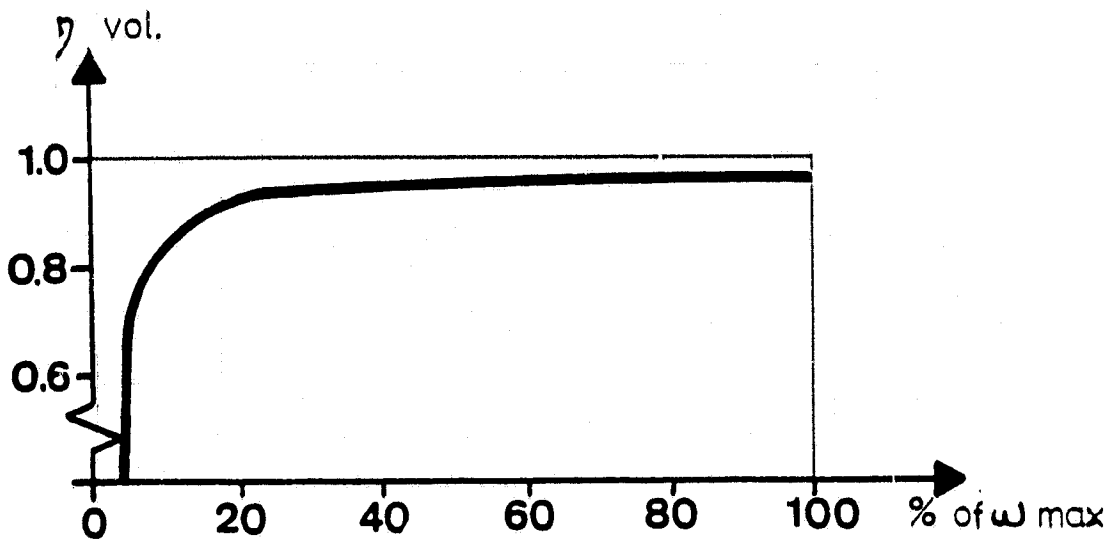


Fig. 8. Qualitative relationship $\eta_{vol}$ vs. $\omega$

- At any reasonable operating speed $\omega$ and differential
  pressure $\Delta p$, the total efficiency $\eta_{tot}$ decreases to
  zero in the low displacement regime (cf. F 9). The
  reason is that some basic losses are fixed, while the trans-
  mitted useful power is decreasing.
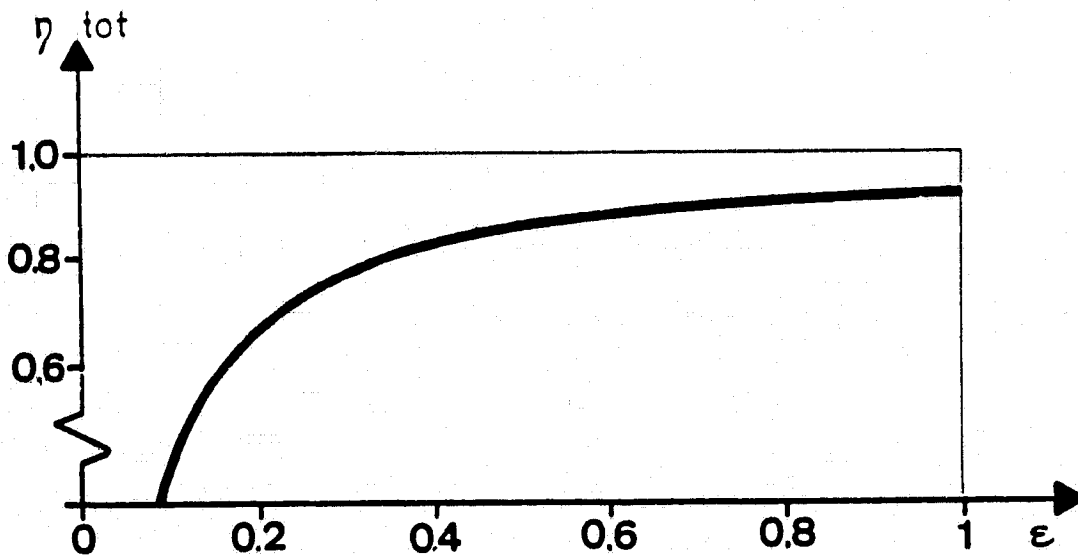


Fig. 9. Qualitative relationship $\eta_{tot}$ vs. $\varepsilon$

From the diagrams in Figs. 7 through 9 can be concluded that operation within any of the low-value regimes, $<10\%$, of the maximum speed, pressure, and displacement, causes considerable losses, $\eta < 80\%$, and should thus be avoided, if possible.

A detailed discussion and quantification of the losses will be given in Chapter 6.

## 4. AVAILABLE DESIGN CONCEPTS

The design problem consists of converting a constant hydrostatic pressure into a variable driving force, covering the range of 0 through approximately 5000 N at any peripheral velocity of the driving wheels up to about 30 m/s.

The main control problem is control of the driving force, while vehicle speed is a dependent variable, controlled indirectly via the driving force. This concept may seem unusual in automotive applications. However, it is beneficial in the design of conventional automobile propulsion systems, as well, as advocated by A. Frank et al. *)

In terms of hardware, the problem could be solved in a straightforward manner by a variable-displacement hydrostatic unit connected to the pressurized fluid supply and delivering its torque to the driving wheels via a conventional final drive. Torque control is obtained by controlling the variable displacement.

This solution could be quantified (cf. Eqs. (11) and (13)) to:

$$T = \varepsilon * \eta_{mech} * D'_{max} * \Delta p \qquad (23)$$

where $T$ is the input torque to the final drive, corresponding to any desired driving force $F$, which is controlled by a proper choice of $\varepsilon$.

The size of the hydrostatic motor is then:

$$D'_{max} = T_{max} / (\eta_{mech} * \Delta p) \qquad (24)$$

where $T_{max}$ corresponds to a selected maximum driving force $F_{max}$ (cf. F 5).

However, some alternative concepts also exist. The total displacement $D'_{max}$ could be obtained:

- either as a sum of the displacements of two or more units (some of them having fixed displacements)

---

*) cf. e.g. paper presented at the ASME Power Transmission & Gearing Conference, San Fransisco, Aug. 1980, entitled "Principles and Definitions of Continuously Variable Transmissions with Emphasis on Automotive Applications".

- or by a "magnification" of a basic displacement obtained by connecting a, two- or more speed, reduction gear between the hydrostatic motor and the final gear

- or by a combination of the two abovementioned concepts.

Before listing a number of design concepts that might have a potential of high energy economy, low weight, etc, we will explain two subconcepts, namely, power recirculation and hydraulic polarity shift.

## Power recirculation (PRC)

The interpretation of two hydrostatic motors working in parallel is obvious:
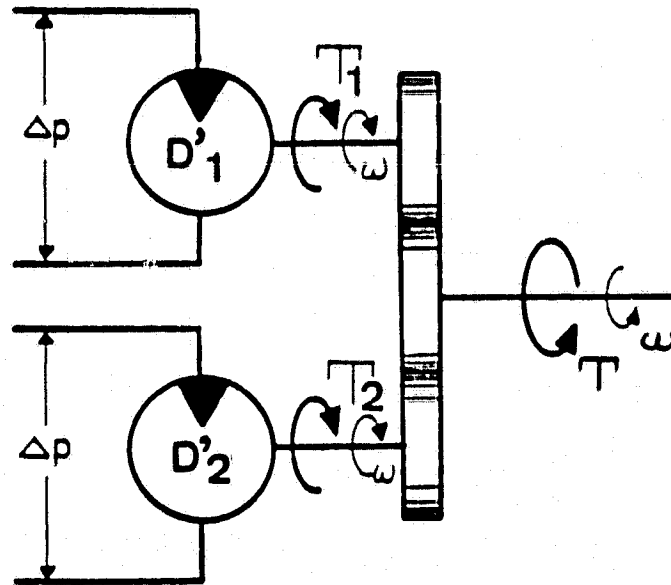
Fig. 10. Scheme of two hydrostatic motors in parallel

$$T_1 = \eta_{mech,1} * D_1' * \Delta p$$
$$T_2 = \eta_{mech,2} * D_2' * \Delta p$$
$$\Rightarrow \text{ assuming } \eta_{mech,1} \cong \eta_{mech,2}$$

$$T = (D_1' + D_2') * \eta_{mech} * \Delta p \tag{25}$$

The question may arise as to whether or not $(D_1' - D_2')$ has a physical interpretation in the context of equations like Eq. (25).

The answer is yes, and the interpretation is that one of the units is operating as a <u>motor</u>, e.g., $D_1'$, and the other, $D_2'$, as a <u>pump</u>. Physically this means that Unit 1 is picking up hydrostatic power from the reservoir and converts it into mechanical power. Thereby some power is lost (friction and leakage).

Part of the mechanical power passes to the output shaft without special losses.

The remaining mechanical power is <u>recirculated</u> to the hydrostatic reservoir via Unit 2, whereby some additional power is lost (friction and leakage).

Analytically the situation is described as follows:

$$T_1 = \eta_{mech,1} * D_1' * \Delta p$$
$$T_2 = D_2' * \Delta p / \eta_{mech,2} \tag{26}$$
$$T = T_1 - T_2$$

$$q_1 = \omega * D_1' / \eta_{vol,1}$$
$$q_2 = \omega * D_2' * \eta_{vol,2} \tag{27}$$

The net output power is
$$P_{out} = T * \omega = (\eta_{mech,2} * D_1' - D_2' / \eta_{mech,2}) \cdot \Delta p * \omega \tag{28}$$

and the net input power is
$$P_{in} = (q_1 - q_2) * \Delta p = (D_1' / \eta_{vol,1} - D_2' * \eta_{vol,2}) * \omega * \Delta p \tag{29}$$

which could be combined to a total net efficiency:

$$\eta_{tot} = P_{out}/P_{in} = (\eta_{mech,1} - \theta/\eta_{mech,2})/(1/\eta_{vol,1} - \theta * \eta_{vol,2}) \tag{30}$$

where $\theta = D_2'/D_1' < 1$

An evaluation of Eq. (30) shows that the total efficiency at PRC always is lower than the efficiency for one single unit transmitting the output power.

The PRC characteristics can be explained semi-quantitatively
by a comparison of different solutions to the following basic
problem:

A variable output torque is to be produced within the range
$0 \leq T \leq T_{max}$, utilizing a given constant differential pressure
$\Delta$ p. For the sake of simplicity, the output speed $\omega$ will
be considered constant.

a) A straightforward solution is to use a variable displacement
   motor, the displacement of which is calculated according to
   Eq. (24). The output torque is controlled by the fractional
   displacement $\varepsilon$ .

b) A simple, but energy-wasting solution is to use a fixed
   displacement motor and to reduce continuously the input
   pressure $\Delta$p to zero by means of a variable throttle between
   the fluid reservoir and the motor.

c) One variable displacement unit and one fixed displacement
   unit are used, both with a displacement that is half of
   the displacement used in a) and b) above. Both units are
   active for all required torques, the fixed displacement
   unit operating as a motor the whole time, and the variable
   machine operating as a pump in the low-torque regime
   - leading to PRC - and as a motor in the high-torque regime.

d) One fixed and one variable displacement motor of the "half"
   size as in c) are used. In the low-torque regime the variable
   motor is used alone. In the transition to the high-torque
   regime, the fixed motor is connected to the fluid supply,
   at the same time as the displacement fraction $\varepsilon$ for the
   variable motor is changed instantaneously from 1 to 0.
   Higher  torques are then obtained by increasing the amount
   of $\varepsilon$ .

The relative power loss for a variable displacement machine,
$\Delta P/P_{max,out}$, is shown in Fig. 11, where the absolute power
loss, $\Delta P$, due to leakage and friction is related to the output
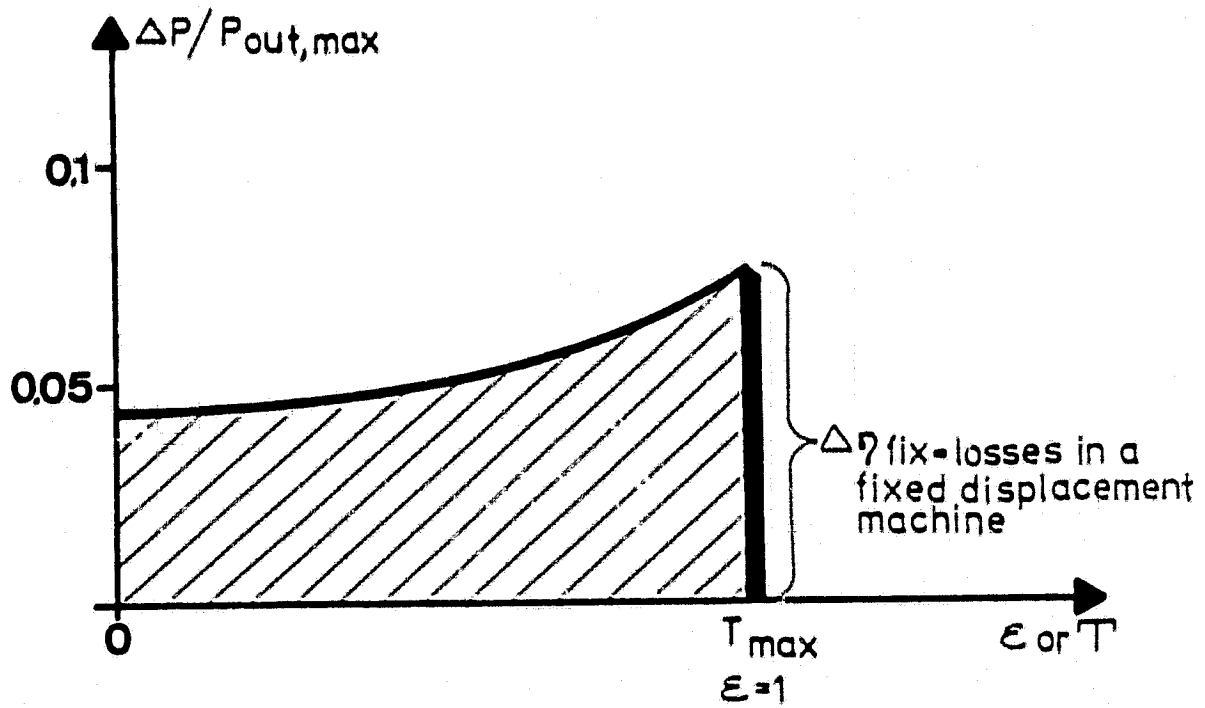power at the maximum displacement.

Fig. 11. Relative power loss for a variable displacement
machine, pertaining to case a).

As will be shown later, the relative losses are almost inde-
pendent of size. Thus, loss diagrams could be composed for the
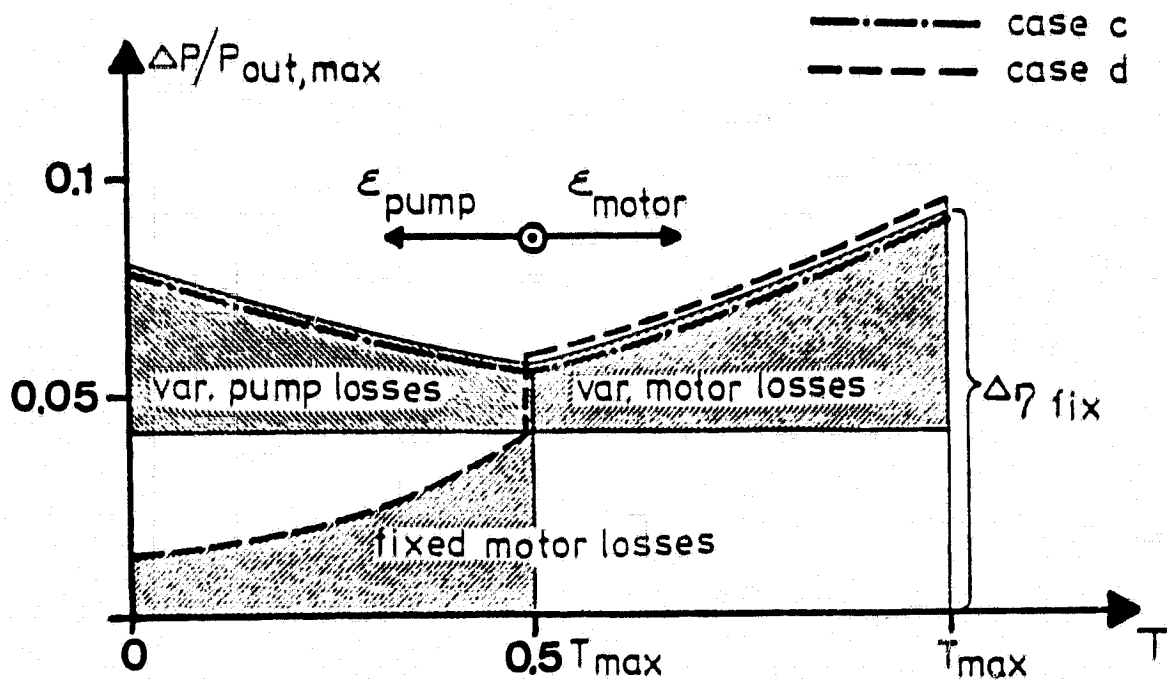cases c) and d) (cf. F 12).



Fig. 12. Relative losses in two-unit arrangements.

At throttling, case b), the power input is constant at all output torques. Most of the power is therefore lost as internal friction in the fluid (cf. F 13).
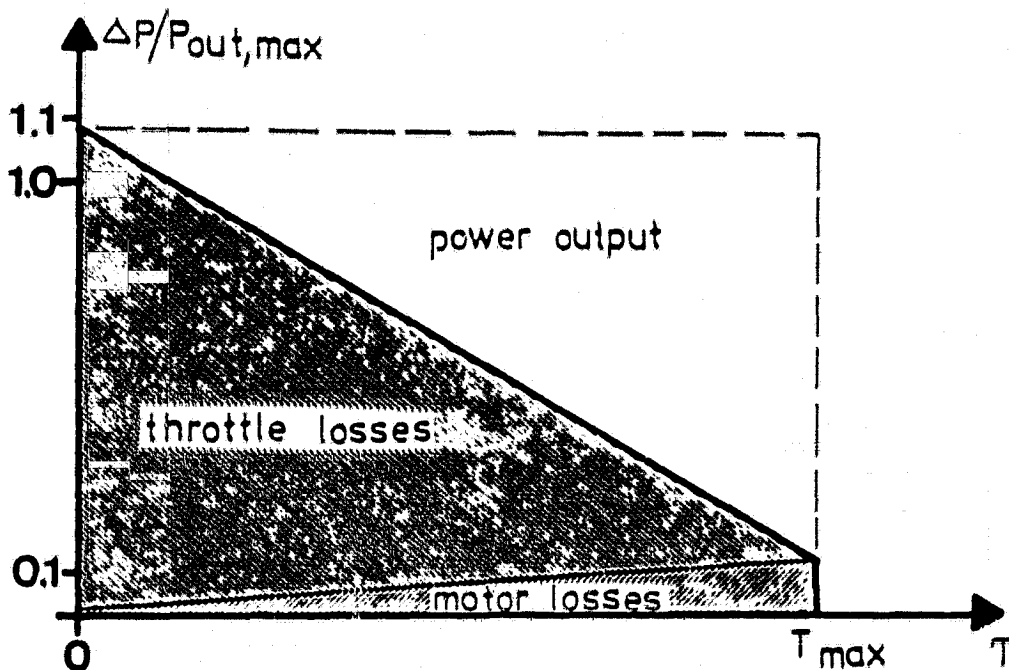


Fig. 13. Losses in a throttled system

The following conclusions can be made:

- losses are higher at PRC than in comparable systems with a straight power flow [case c) vs. cases a) and d)]

- losses are of the same order of magnitude for one large <u>motor</u> or several small <u>motors</u> in parallel [case a) vs. d)]

- losses are very high at torque control by throttling of fixed displacement motors [case b)]

- at very low torque output the mutual power loss is related for the cases a):c):d) as 2:4:1

- PRC is not justified by low-loss considerations; however, it offers a smooth shift between different modes of operation.

## <u>Hydraulic polarity shift (HPS)</u>

The change of mode of operation from full displacement pump to full displacement motor may be obtained in one of two ways for the case with unchanged direction of rotation:

- by a continuous change of $\mathcal{E}$ from one extreme (+1) via zero
  to the other extreme (-1), whereby the direction of flow, q,
  is changed continuously during the mechanical motion
  $\alpha \rightarrow 0 \rightarrow -\alpha$; the change may be completed in about 1 s

- by shifting - by valve operation - the hydraulic connections
  between the connecting ports and the high- and low-pressure
  reservoirs, respectively, whereby the rigid parts of the
  unit do not change their state of motion (thus no inertial
  forces), but the direction of flow is changed "instantaneously."

## Design concepts considered

The following groups of design concepts have been considered.
1. One single motor
2. Two motors in parallel
3. One single motor with a two-speed transmission
4. Other compound systems of some merit

Groups 2 and 4 contain the following alternatives:

2a. Either one of two variable motors in operation
2b. Either one or both of two variable motors in operation
2c. One fixed and/or one variable motor in operation
2d. One fixed motor and/or one variable motor with PRC and HPS
2e. One fixed motor with HPS and/or one variable motor with PRC

4a. One single variable motor and a three-speed transmission
4b. One fixed and/or one variable motor with a two-speed
    transmission
4c. Two fixed motors and/or one variable motor
4d. Two fixed motors and/or one variable motor with PRC and HPS

All considered concepts have the potential of access to all
driving forces $F \leq F_{max}$, hydraulic reverse gear, and recovery
of braking energy.

In Appendix 1 are given the schemes of the main configurations
of the different concepts and relevant control strategies,
F vs. $\mathcal{E}$ . It should be noted that the control strategies serve
only as examples, using assumed (not optimized) displacements
and gear ratios. As a common frame of reference the following
is used:

$$F_{max} = 6000 \text{ N}$$

$$F_{urban} \leq 2500 \text{ N} \quad \text{(light grey)}$$

$$F_{h-way} \leq 600 \text{ N} \quad \text{(dark grey)}$$

(31)

The F values in Eq. (31) are based upon Fig. 5, modified and adjusted according to experience and engineering intuition.

All the design concepts include other hardware in addition to that given in Appendix 1. Such components, e.g. a final transmission, flow control valves, hoses, micro-processor and other control components, are approximately of the same size, weight, and performance. Therefore, they have not been included in the sizing and optimization process.

# 5. RECOMMENDED DESIGN CONCEPTS

When evaluating the total merits of the candidate systems
described in the preceding section, one should consider the
following parameters:

- size of the variable motor/pump
- number of significant components
- number and character of gear shifts
- regime of $\varepsilon$ used in urban/highway driving
- possible power recirculation (PRC) in urban/highway driving

The motor size is considered in terms of transmitted power,
which presumes that both the maximum pressure and the maximum
speed will be utilized in the optimized design. It is possible
to meet any motor output speed by a proper choice of transmission
ratios of the final and any intermediate mechanical transmission.

The character of the gear shifts - especially the time involved -
varies among the systems described. The clutch operation and
change of hydraulic polarity (HPS) are completed quickly;
the change of displacement from one extreme to the other re-
quires significantly longer time.

The fuel economy is influenced by the regime of $\varepsilon$ that is most
frequently used, as well as by possible power recirculation (PRC)
under frequently used driving conditions.

It is assumed [cf. Eq. (31)] that urban driving requires up to
about 40% and highway driving 10% of the maximum driving force.
If low displacement ($\varepsilon < 0.20$) or PRC occur in these operating
regimes ($F < 10\%$ and 40% of $F_{max}$, respectively), a significant
increase of losses will result.

Parameters of importance for the evaluation are listed in Table 1.

TABLE 1. Comparison of various design concepts

| System type | 1 | 2 | | | | | 3 | 4 | | | |
|---|---|---|---|---|---|---|---|---|---|---|---|
| | | a | b | c | d | e | | a | b | c | d |
| Size of var.machine | 1.0 | 0.8 | 0.67 | 0.5* | 0.33 | 0.67 | 1.0 | 1.0* | 0.5* | 0.25 | 0.14 |
| No. of var.machine | 1 | 2 | 2 | 1 | 1 | 1 | 1 | 1 | 1 | 1 | 1 |
| No. of fixed machine | 0 | 0 | 0 | 1 | 1 | 1 | 0 | 0 | 1 | 2 | 2 |
| No. of clutches | 0 | 2 | 2 | 1 | 1 | 1 | 1 | 2 | 2 | 2 | 2 |
| No. of gear meshes | 0 | 1 | 1 | 1 | 1 | 1 | 2 | 2 | 2 | 2 | 2 |
| No. of fast shifts | 0 | 1 | 2 | 0 | 1 | 0 | 0 | 0 | 0 | 3 | 3 |
| No. of slow shifts | 0 | 0 | 0 | 1 | 0 | 2 | 1 | 2 | 3 | 0 | 0 |
| PRC/urban | 0 | 0 | 0 | 0 | 0 | yes | 0 | 0 | 0 | 0 | yes |
| PRC/h-way | 0 | 0 | 0 | 0 | 0 | yes | 0 | 0 | 0 | 0 | no |
| Low $\varepsilon$/urban | yes | 0 | 0 | ? | 0 | 0 | 0 | 0 | 0 | 0 | yes |
| Low $\varepsilon$/h-way | yes | 0 | 0 | yes | 0 | 0 | 0 | 0 | 0 | 0 | 0 |
| Magnitude of complexity | 0 | 0 | 0 | 1 | 1 | 1 | 0 | 0 | 1 | 2 | 2 |

*) might be slightly reduced when a reduced driving force is accepted in the high speed regime of the vehicle.

A fully formalized selection of the most promising design concepts seems to be impossible. Some parameters are very difficult to quantify, such as complexity, riding comfort (jerks when gears are shifted), and reliability.

The first screening of candidate systems must to a great extent be done by engineering experience and intuition, which are difficult factors to incorporate into a computerized analysis of the systems.

24

A design concept with a high potential should meet the
following criteria:

- only one variable displacement machine (heavy and expensive)
- smallest possible displacement for the variable machine (heavy
  and expensive)
- maximum two hydrostatic machines in all (i.e., the second one
  should be a fixed displacement machine) (complexity)
- low yoke angles (low $\varepsilon$ ) and PRC should be avoided as far as
  possible under normal driving conditions (high losses)
- the number of shifting points (discontinuous changes) should
  be minimized and the duration of the shifting procedure should
  be as short as possible (in order to make the ride comfortable).

None of the reviewed systems meets all the criteria mentioned
above. Some systems are ruled out immediately, among them the
single variable motor, which at normal driving conditions
essentially has to operate in the low yoke angle regime.

The following two systems have been selected for further detailed
analysis and optimization:

A: One variable displacement V-20 motor and a two-speed planetary
   gear train in series in front of the final gear (equivalent
   to Case 3 in Table 1) (cf. F 14).
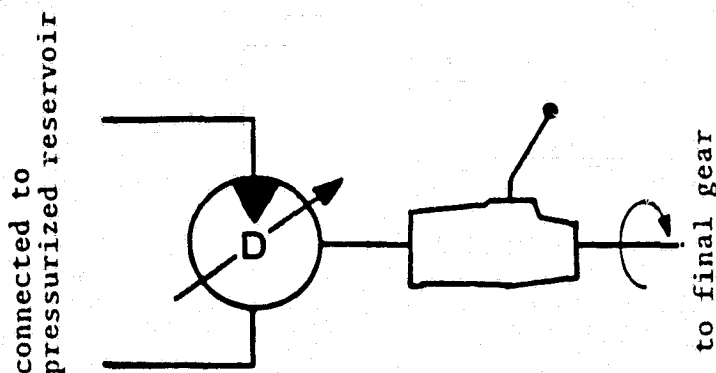


D= variable motor of type V-20

Fig. 14. Fundamental design concept of system A.

B: One variable displacement V-20 motor/pump in parallel with
a disconnectable fixed displacement motor, both in front of
the final gear (equivalent to Case 2d in Table 1) (cf. F 15).
At low required driving force, the variable machine operates
as a motor only. At an increased driving force (about 1/3 of
$F_{max}$), the fixed motor is connected to the system and the
variable machine is by HPS shifted to pump operation,
whereby PRC conditions occur. At still higher driving force
(2/3 of $F_{max}$), the V-20 machine changes to the motor opera-
tion mode.
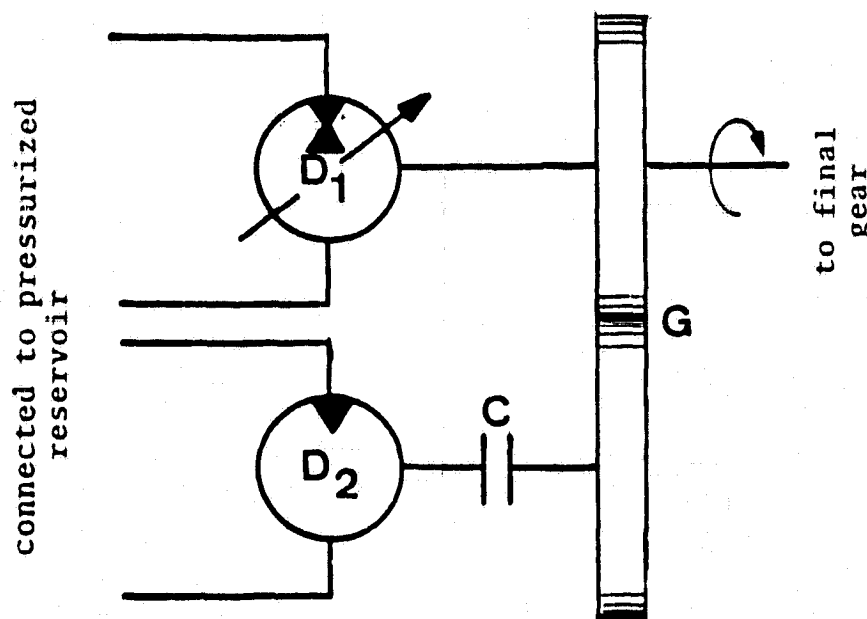


$D_1$ = variable motor/pump of type V-20
$D_2$ = fixed motor of type F-11
$G$ = gearbox, constànt ratio
$C$ = clutch

Fig. 15. Fundamental design concept of system B.

N.B. System B may deliberately change towards system 2c in
Table 1 if the optimization procedure is given full free-
dom. The displacements are then oversized, and the shift
points are chosen in such a way that PRC is partly or
fully avoided.

# 6. MODELING OF HYDROSTATIC COMPONENTS

## General approach

Volvo Flygmotor has extensive experience with fixed displacement F-11 series pumps/motors. Performance data have been obtained for a variety of sizes.

The first type of variable displacement machines marketed by Volvo Flygmotor was the V-30 series of in-line machines. The design concept and thus also the performance, are to some extent different from those of the F-11 series of machines. Performance data is available from three different sizes of machines.

Later a variable displacement version of the F-11 series, named V-20, was developed. One basic size, $D = 137$ cm$^3$/rev, has been marketed since 1974. An updated version of the basic machine with the displacement $D = 180$ cm$^3$/rev has been developed quite recently and tested within this program.

All experience gained hitherto matches quite well the general theoretical description of losses in hydrostatic machinery which has been developed for the middle and full load operating regimes. There is a shortage of performance data on the low-load operating regime, and a special theory describing the losses needs to be developed as well. However, the middle and full-load theory covers the low-load regime with acceptable accuracy.

The state of the art of modeling losses in hydrostatic pumps/motors defines torque losses $\Delta T$ and leakage losses $\Delta q$ as follows: *)

for motors:

$$T_{out} = T_{theor} - \Delta T = D' * \Delta p_{in} - \Delta T \tag{32}$$

$$q_{in} = q_{theor} + \Delta q = D' * \Delta p_{in} + \Delta q \tag{33}$$

for pumps:

$$T_{in} = T_{theor} + \Delta T = D' * \Delta p_{out} + \Delta T \tag{34}$$

$$q_{out} = q_{theor} - \Delta q = D' * \Delta p_{in} - \Delta q \tag{35}$$

---

*) Johansson, Ingvar & Larsson, Gunnar: Analysis of the efficiency of a hydraulic axial piston machine, M.Sc. thesis (in Swedish), Chalmers Univ. of Technology, Dept. of Mechanical Engineering (Machine Elements), 1967.

$\Delta$ T and $\Delta$ q are assumed to consist of a number of partial losses, each of which is related to some identified physical phenomenon and thus proportional to some externally measurable parameter.

The various loss sources are:

- Parasitic torque loss (PTL)
  $$\Delta T = \text{const. (for a given machine)} \tag{36}$$

- Dry friction (DF)
  $$\Delta T \sim p_{equ} \tag{37}$$

- Viscous friction (VF)
  $$\Delta T \sim \mu * \omega \tag{38}$$

- Turbulent flow resistance (TFR)
  $$\Delta T \sim \varrho * \omega^2 \tag{39}$$

- Viscous clearance leakage (VCL)
  $$\Delta q \sim p_{equ}/\mu \tag{40}$$

- Compressibility (C)
  $$\Delta q \sim \Delta p * \omega \tag{41}$$

As can be seen from Eqs. (36) through (41), the losses are proportional to some of the parameters load ($\Delta$ p or $p_{equ}$), speed ($\omega$), density ($\varrho$), and viscosity ($\mu$).

The load parameter appears as $\Delta$ p (=differential pressure) and $p_{equ}$. The equivalent pressure, $p_{equ}$, is introduced to take care of the back pressure, $p_{back}$, where adequate.

In most applications $p_{back}$ is negligible; then $p_{equ} \simeq \Delta p$.

If, however, $p_{back}$ is not negligible, it contributes to dry friction and viscous clearance leakage losses. Furthermore, $\Delta$ p is active only over one half of a revolution, but $p_{back}$ is active over the full revolution. Therefore, the "double" influence of $p_{back}$ is taken into account as follows:

$$p_{equ} = \triangle p + 2*p_{back} \tag{42}$$

The experimental experience of the F-11 type of machines indicates that the relative losses are independent of the size of machines over a broad range of displacements. This fact could be used in a general type of loss expressions:

$$\triangle T = D'*(C_{PLT}+C_{DF}*p_{equ}+C_{VF}*\mu*\omega+C_{TFR}*\zeta*\omega^2) \tag{43}$$

$$\triangle q = D'*(C_{VCL}*p_{equ}/\mu+C_c*\triangle p*\omega) \tag{44}$$

The loss expressions could be converted into efficiency expressions as follows:

for motors:

$$\eta_{vol} = "q_{out}"/q_{in} = q_{theor}/(q_{theor}+\triangle q)=1/(1+\triangle q/(D'*\omega)) \tag{45}$$

$$\eta_{mech} = T_{out}/"T_{in}" = (T_{theor}-\triangle T)/T_{theor}=1-\triangle T/(D'*\triangle p) \tag{46}$$

for pumps:

$$\eta_{vol}=q_{out}/"q_{in}" = (q_{theor}-\triangle q)/q_{theor}=1+\triangle q/(D'*\omega) \tag{47}$$

$$\eta_{mech} = "T_{out}"/T_{in}=T_{theor}/(T_{theor}+\triangle T) = 1/(1+\triangle T/(D'*\triangle p)) \tag{48}$$

If the above expressions are used at low load and speed conditions, the best fit of the coefficients $C_{PLT}$, $C_{VLC}$, etc. to experimental data yields numerically different values of the coefficients at motor and pump operation respectively. Thus, the limit values of $\triangle T$ and $\triangle q$ will not be equal for the pump and motor case when $\triangle p$ and $\omega$ approach zero.

This discrepancy is, however, of lesser practical importance. It could probably - if necessary - be overcome by developing the state-of-the-art of the loss theory through splitting the load losses into $\triangle T$ and $\triangle(\triangle p)$ and the speed losses into $\triangle q$ and $\triangle \omega$

## F-11 machines

The following loss models developed by Volvo Flygmotor prior
to the present project have been used:

pump:

$$\Delta T = D' * (1.42*10^5 + 5.592*10^{-3}*p_{equ}) \tag{49}$$

$$\Delta q = D' * (1.78*10^{-8}*p_{equ} + 8.74*10^{-10}*\omega*\Delta p) \tag{50}$$

motor:

$$\Delta T = D' * (3.30*10^5 + 8.96*10^{-3}*p_{equ}) \tag{51}$$

$$\Delta q = D' * (3.92*10^{-8}*p_{equ} + 3.50*10^{-10}*\omega*\Delta p) \tag{52}$$

The above coefficients are obtained for a fluid with
$\mathcal{S} = 860$ kg/m$^3$ and $\mu = 0.026$ Ns/m$^2$. The coefficients may be
modified to apply to other viscosities, as indicated in
Eq. (44).

The estimation of weight, volume, and maximum speed is
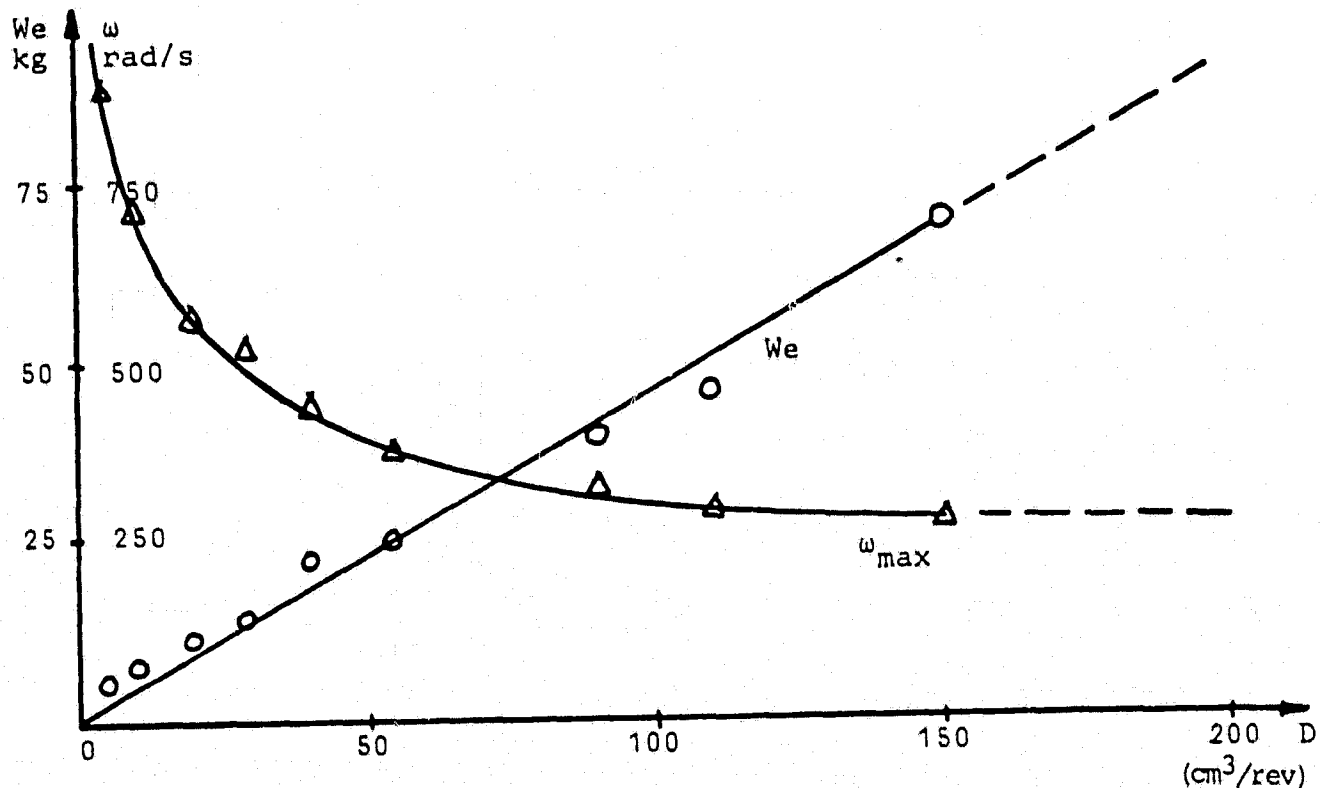based upon trend curves for F-11 machines. (cf. F 16).



Fig. 16. F-11 series - trends for weight and speed

The data points in Fig. 16 represent a mixture of points from basic and updated designs. An almost linear relationship still exists between the weight We and the displacement, expressed as

$$We = D * 0.47 * 10^6 \quad (kg) \tag{53}$$

The package volume is difficult to define uniquely. However, the density of an enveloping cube is approximately 2750 kg/m$^3$; thus, the volume Vo can be written,

$$Vo = D * 0.17 * 10^3 \quad (m^3) \tag{54}$$

The maximum speed is modeled as

$$\omega_{max} = 4.0 * 10^{-3}/D + 240 \quad (1/s) \tag{55}$$

## V-20 machines, experiments

The modeling of losses in the variable-displacement V-20 series of machines is based on a series of performance tests with special emphasis on operation at low yoke angles (low $\varepsilon$ ) and low speeds ($\omega$) as well as at elevated back pressure.

A back-to-back testing technique (PRC) has been used. A circuit diagram of the performance test setup is shown in Fig. 17. The quantities measured were:(items 1 through 5 refer to meter positions, cf. F 17.

| | | |
|---|---|---|
| 1. Torque, | 10 through 100 Nm | $\pm$ 2% through $\pm$ 1% [*] |
| | 100 through 1000 Nm | $\pm$ 1% through $\pm$ 0.5% |
| 2. Pressure, | 2.5 through 10 MPa | $\pm$ 3% through $\pm$ 1% |
| | 10 through 40 MPa | $\pm$ 1% through $\pm$ 0.25% |
| 3. Flow, | 0.17 through 7.6 $* 10^{-3}$ m$^3$/s | $\pm$ 0.5% |
| 4. Speed, | (any) $\pm$ 0.5% | |
| 5. Temperature, | (any) $\pm$ 1$^\circ$C | |

[*] the given measuring accuracy is assumed to change linearly over the given measuring regime.

TABLE 2. Legend to Fig. 17.

| | |
|---|---|
| ⊕ | Electric Motor |
| ◔ | Oneway Pump with Fixed Displacement |
| ⊘ | Pump/Motor with Variable Displacement |
| ⊘ | Twoway Variable Displacement Pump |
| ◑ | Twoway Motor with Fixed Displacement |
| ⊘ | Volume Flow Meter |
| ⊖ | Thermometer |
| ⊘ | Pressure Gauge |
| | Adjustable Max.Pressure Limiter |
| ◇ | Cooler |
| ◇ | Filter or Strainer |
| ◁ | Non-Return Valve |
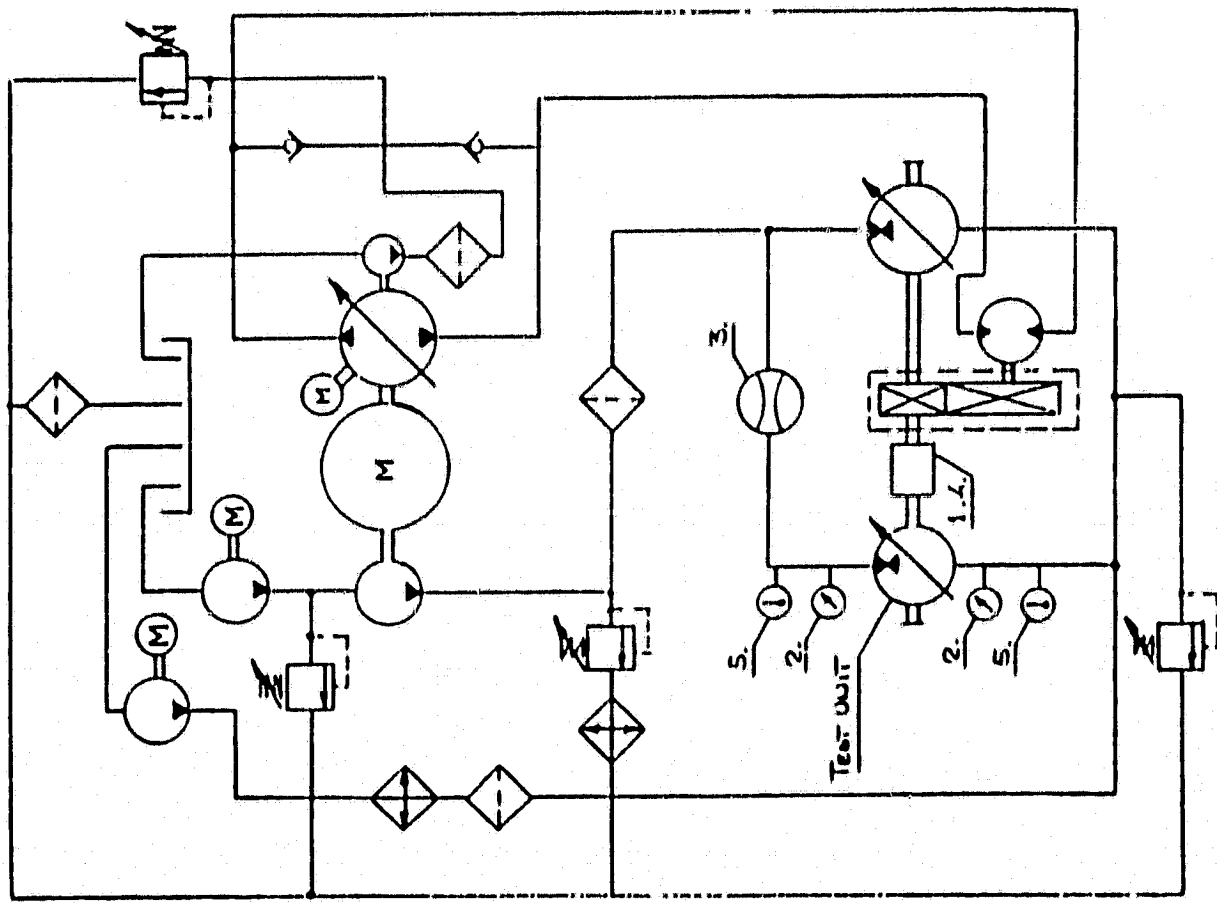


Fig. 17. Circuit diagram of the performance test setup.

Measurements have been carried out for the following matrix
of parameters:

pump_operation

$\triangle$ p: 0,  5,  15,  25,  and  35 MPa
n ($\rightarrow \omega$): 500,  1500,  2000,  2500, and 3000 rpm
$\alpha (\rightarrow \varepsilon$): 40,  25,  15,  10,  6, and $3^{\circ}$

motor_operation

$\triangle$ p: 0,  5,  15,  25,  and  35 MPa
n ($\rightarrow \omega$): 100,  200,  500,  1500,  2000,  2500, and 3000 rpm
$\alpha (\rightarrow \varepsilon$): 40,  25,  15,  10,  6,  4,  and $3^{\circ}$


All tests above were run at $p_{back}$ = 1 MPa, $\varrho$ =860 kg/m$^3$ and
$\mu$ = 0.026 Ns/m$^2$
(Shell Tellus 46 oil at $50^{\circ}$C)

Special tests were performed with elevated temperature and
increased back pressure, respectively, for the following
reduced matrix of paramters:

$\triangle$p: 5,  15,  25 (and 35) MPa
n ($\rightarrow \omega$): 500 and 2500 rpm
$\alpha (\rightarrow \varepsilon$): 25 and $10^{\circ}$

back pressure 10 MPa at t = $50^{\circ}$C, and
temperature $70^{\circ}$C at $p_{back}$ = 1 MPa

Results of the tests, expressed as efficiencies, are given
in Appendix 2.

## V-20 machines, mathematical model

The mathematical model has been developed in the following way:
Experimental data has  been transformed to the form:

$\triangle$ T and  $\triangle$q
as a function of
$\varepsilon$, $\omega$,  $\triangle$ p (and $p_{back}$)

For each $\varepsilon$, data has  been plotted in various ways in order
to refine and identify each of the losses given in Eqs. (36)
through (41). The coefficients $C_{PTL}$, $C_{VCL}$, etc. were thus
obtained as functions of $\varepsilon$.

The influence of the variable displacement $\xi$ was then taken into account purely numerically, by fitting a third order polynomical of $\xi$ to $C_{PTL}$, $C_{VCL}$, etc. Some of the polynomial terms vanished.

The remaining terms give the following loss expressions:

$$\Delta T = D'_{max} * [ (C_1 + C_2 * \xi) + (C_3 * \xi + C_4 * \xi^2 + C_5 * \xi^3) * \omega^2 +$$

$$+ (C_6 + C_7 * \xi) * \omega + (C_8 + C_9 * \xi + C_{10} * \xi^2 + C_{11} * \xi^3) * p_{equ}] \tag{56}$$

$$\Delta q = D'_{max} * [ C_{12} * p_{equ} + (C_{13} + C_{14} * \xi + C_{15} * \xi^2 + C_{16} * \xi^3) *$$

$$* \omega * \Delta p] \tag{57}$$

Separate sets of $C_1$ through $C_{16}$ for pump operation, $c^p$, and motor operation, $c^m$, are listed in Table 2. The fractional displacement $\xi$ is in both cases positive.

TABLE 2. Loss coefficients for pump and motor operation.

| Type of loss | Subscript (Index) | $C^p$ | $C^m$ |
|---|---|---|---|
| Parasitic torque | 1 | $2.12 * 10^5$ | $1.23 * 10^5$ |
| | 2 | $-0.706 * 10^5$ | $-0.706 * 10^5$ |
| Turbulent flow resistance | 3 | 1.66 | -6.20 |
| | 4 | 6.00 | 23.63 |
| | 5 | 3.84 | -10.51 |
| Viscous friction | 6 | $1.10 * 10^3$ | $1.24 * 10^3$ |
| | 7 | $1.10 * 10^3$ | $1.59 * 10^3$ |
| Dry friction | 8 | $9.53 * 10^{-3}$ | $8.21 * 10^{-3}$ |
| | 9 | $3.53 * 10^{-3}$ | $-2.72 * 10^{-3}$ |
| | 10 | 0 | $80.16 * 10^{-3}$ |
| | 11 | 0 | $-49.28 * 10^{-3}$ |
| Viscous leakage | 12 | $6.00 * 10^{-8}$ | $6.00 * 10^{-8}$ |
| Compressibility | 13 | $4.62 * 10^{-10}$ | $4.33 * 10^{-10}$ |
| | 14 | $0.95 * 10^{-10}$ | $3.77 * 10^{-10}$ |
| | 15 | $13.41 * 10^{-10}$ | $-4.70 * 10^{-10}$ |
| | 16 | $-12.27 * 10^{-10}$ | 0 |

The coefficients in Table 2 are calculated for a fluid with
$S = 860$ kg/m$^3$ and $\mu = 0.026$ Ns/m$^2$.
They may be modified to apply to other densities and vis-
cosities as indicated in Eqs. (43) and (44).

The accuracy of the numerical loss model is in most cases
within the limits of experimental errors embedded in the data
used. At full load there may be errors of $\pm$ 1% in both $\eta_{vol}$
and $\eta_{mech}$. As the absolute errors are of the same order of
magnitude, the relative errors increase with decreasing load,
making the $\eta$ predictions uncertain in the low-power regime
(< 10% of maximum power).

The modeling of weight, size, and maximum speed is of necessity
based upon a limited and inhomogeneous number of data for
variable displacement machines. Only three units exist of the
V-30 series and 2 units of the V-20 series. In each series
one unit is of an updated design, the others of the basic
design. Existing data are plotted in F 18.
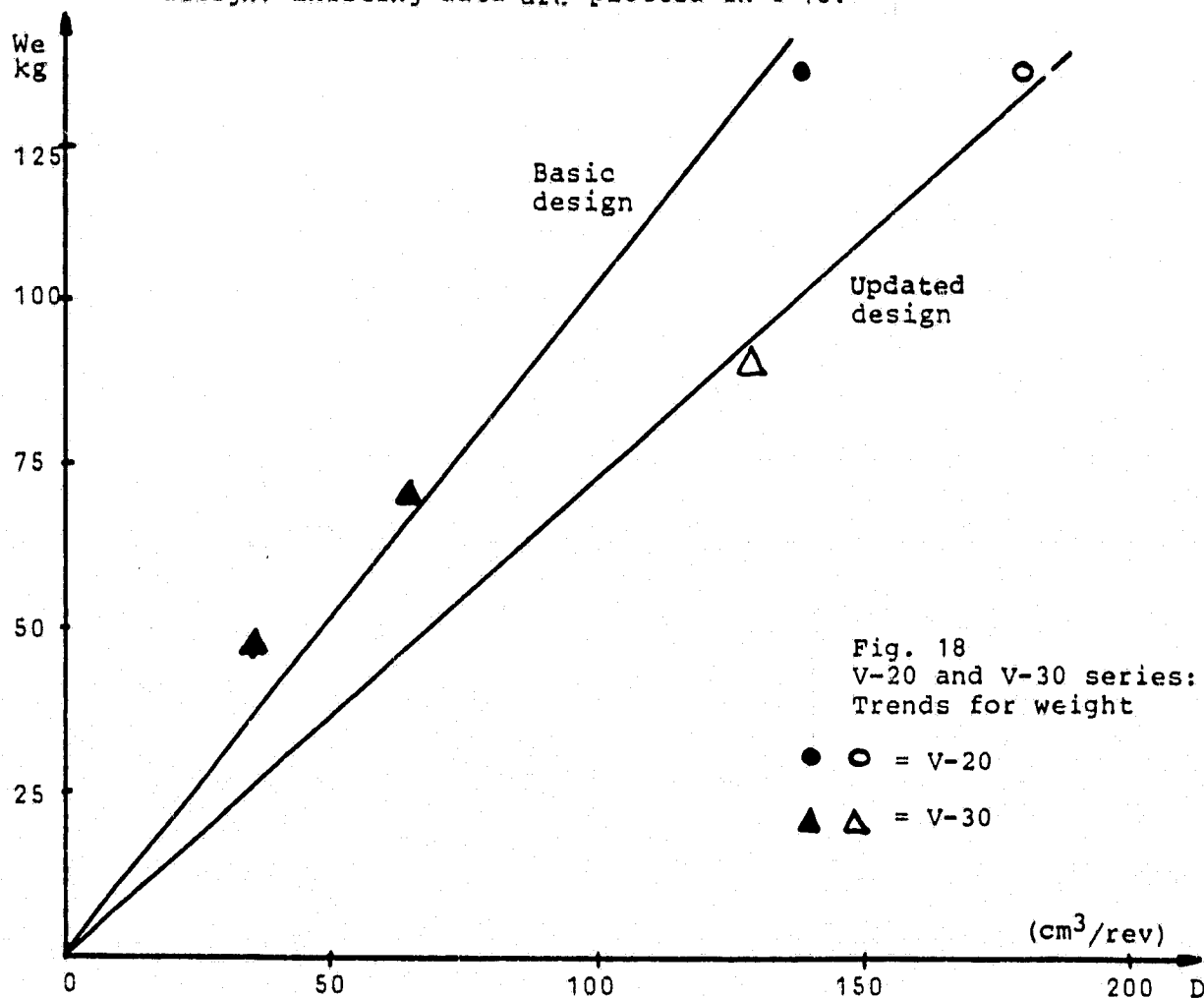


Fig. 18
V-20 and V-30 series:
Trends for weight

● ○ = V-20

▲ △ = V-30

If the well-documented trends for the F-11 series machines
are used (cf. Fig. 16 and Eqs. (53) and (55)), the models
for V-20 series machines could be based upon these trends
and the data for the V-20-180 updated machine only, yielding

$$We = D*0.75*10^6 \qquad (kg) \tag{58}$$

$$Vo = D*0.45*10^3 \qquad (m^3) \tag{59}$$

$$\omega_{max} = 4.0*10^{-3}/D+300 \quad (1/s) \tag{60}$$

## 7. MODELING OF GEARED COMPONENTS

The following significant geared components are parts of the transmission systems A and B and contribute to the power loss:

- fixed-ratio gear transmission
- two-speed planetary gear train
- final gear of the conventional type
- (clutch)

Other components, such as valves, hoses, fluid reservoirs, filters, coolers, and control equipment, are assumed not to influence the transmission characteristics appreciably. Also their weight and volume might be expected to be the same for various system configurations. Therefore, they are not modeled and not incorporated in the numerical evaluation and optimization procedure.

When modeling power losses for mechanically geared transmissions, one must consider the following types of losses. *)

### Torque losses
$\Delta T$ = const.: idling/parasitic loss
$\Delta T \sim T$: load proportional/gear mesh loss

### Speed losses
$\Delta \omega \equiv 0$ : no losses/positive action.

The significant geared components are modeled numerically as follows:

### Fixed-ratio gear transmission
The transmission ratio, denoted $R_{conn}$, gives the theoretical speed and torque conversion relationships

$$\omega_{out} = \omega_{in}/R_{conn} \tag{61}$$

$$T_{out, theor} = T_{in} * R_{conn} \tag{62}$$

---

*) Mägi, M: On the Efficiencies of Mechanical Co-Planer Shaft Power Transmissions, Diss. Chalmers Univ. of Technology, Gothenburg, Sweden, 1974.

Due to idling and gear-mesh losses, the real torque output
is modified to

$$T_{out} = (T_{in} - \Delta T) * R_{conn} * \eta_{mech} \qquad (63)$$

Numerical loss coefficient values are given in Table 3.

The weight and volume are assumed to be constant because
the maximum transmitted power is constant (cf. Table 3).

N.B. When the transmission is disconnected from the fixed
    displacement machine, the load-dependent gear-mesh
    losses disappear, but the idling losses are still
    affecting the output torque (cf. the position of the
    clutch in Fig. 15).

Two-speed planetary gear train

At direct gear the transmission ratio is unity; the speed
reduction gear has the ratio $R_{low}$, giving the theoretical
speed and torque conversion relationships for the low gear:

$$\omega_{out} = \omega_{in} / R_{low} \qquad (64)$$

$$T_{out,theor} = T_{in} * R_{low} \qquad (65)$$

Due to idling and gear mesh losses, the real torque output
is modified to

$$T_{out} = (T_{in} - \Delta T) * R_{low} * \eta_{mech} \qquad (66)$$

For the direct gear the real output torque is

$$T_{out} = T_{in} - \Delta T \qquad (67)$$

Numerical data on losses and weight/size coefficients are
given in Table 3.

Final gear of the conventional type

This transmission consists of a hypoid gear and a differential
gear in series, converting the rotational mode of motion into
a linear mode of motion at the periphery of the driving wheels.
The transmission ratio R' defines the theoretical speed and
torque relationships. R' is given as the amount of rotation of
the universal shaft (in radians) per traveled distance (in meters),

$$v = \omega_{in}/R' \tag{68}$$

$$F_{theor} = T_{in} * R' \tag{69}$$

Due to idling and gear mesh losses, the real torque output is modified to

$$F = (T_{in} - \Delta T) * R' * \eta_{mech} \tag{70}$$

Numerical data on losses and weight/size coefficients are given in Table 3.

TABLE 3. Loss and weight/size data on geared transmissions.

| Component | $\Delta T$ *) | $\eta_{mech}$ *) | We (kg) **) | Vo (m$^3$) **) |
|---|---|---|---|---|
| Fixed-ratio geared transm. | $0.03*T_{max}$ | 0.97 | 7 | 0.005 |
| Two-speed planetary gear | $0.05*T_{max}$ | 0.96 | $7+0.003*T_{max}$ | 0.004 |
| Final gear | $0.05*T_{max}$ | 0.96 | - | - |
| Clutch | - | - | 3 | 0.003 |

*) Data extracted from: Reichenbächer, H: Gestaltung von Fahrzeuggetriebe, Springer-Verlag, 1955.

**) Data based upon Volvo Car Co. rules of thumb; data contain minimum casing.

## 8. OPTIMIZATION CRITERIA

The contract originally prescribed the highest possible
efficiency at steady-state driving in the speed range of
6.7 through 22.4 m/s and the lowest possible volume, weight,
and complexity as optimization criteria of the system.

Highest possible mean value of the total efficiency over
some steady-state speed regime seems to be an oversimplified
approach to the problem, since the total fuel economy is one
of the main problem areas for road vehicles. The total fuel
economy is, however, strongly linked to the type of driving,
i.e., to some driving cycle.

In the present analysis the fuel economy in a wide sense is
taken as a basis for the optimization of the systems A and B
recommended for further analysis (cf. p. 24 ).

The direct fuel economy is based upon the EPA Urban Driving
Cycle. Indirectly, the package weight increases the rolling
resistance and the inertial load and thus the fuel economy.
Similarly, the package volume increases the front area of the
vehicle and thus the increased drag losses also increase the
fuel consumption.

The complexity of the system (and the cost related thereto),
the reliability, and the driving comfort and other non-
quantitative values have been considered in the preceding
investigation of candidate systems.

The EPA Urban Driving Cycle has been analyzed in detail. The
results are summarized in the Driving Cycle Matrix (cf. F 4).

Another similar matrix may be computed, containing information
on system performance as a function of F and $\dot{v}$. If the system
configuration, component size, and loss models as well as the
control situation are known, it is possible to calculate the
performance characteristics (efficiencies, flows, torques,
etc) for each output condition defined by F and v.

Should two or more control positions (gear in operation and displacement utilized) permit the same output, the control mode having the lowest power loss is chosen. The results are summarized as system characteristics matrices (F 19).
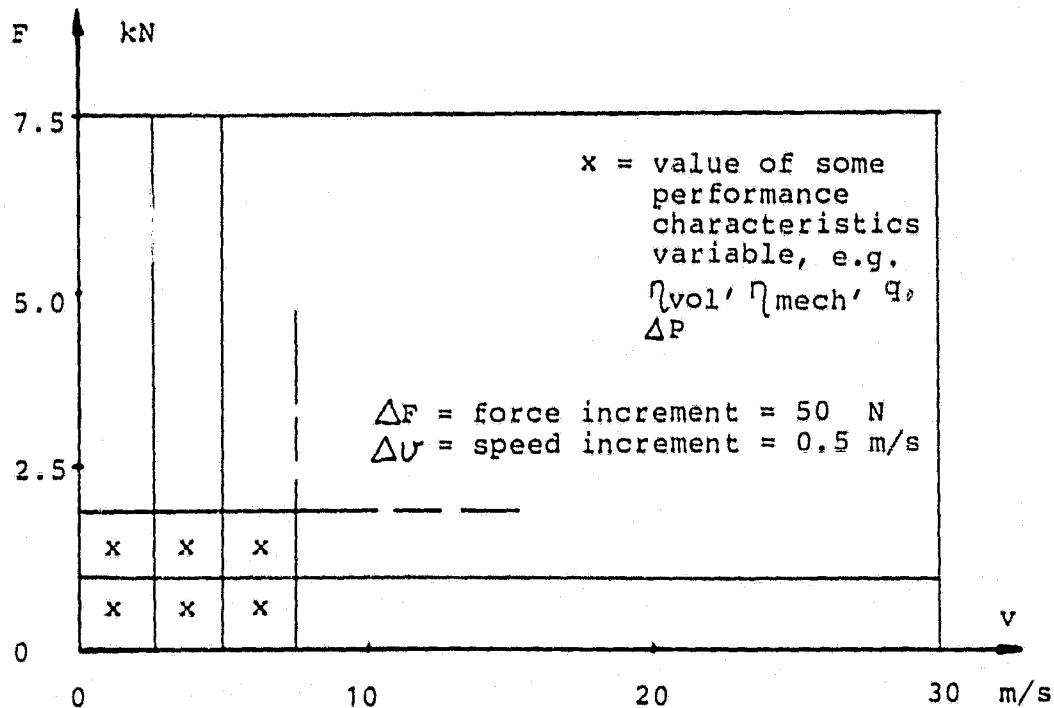
F ▲ kN

7.5 ┤

x = value of some
performance
characteristics
variable, e.g.

5.0 ┤  $\eta_{vol}$, $\eta_{mech}$, $q$,
$\Delta P$

$\Delta F$ = force increment = 50  N
$\Delta v$ = speed increment = 0.5 m/s

2.5 ┤

|   |   |   |
| x | x | x |
| x | x | x |

0  ─────────────────────────────────── v

0          10          20          30  m/s

Fig. 19. System characteristics matrix

The total energy consumed during some specific driving cycle is obtained simply by multiplying the driving cycle matrix and the power input matrix, which is one of the system characteristics matrices.

This kind of energy consumption analysis could be repeated for any system with arbitrarily chosen sizes of components. In addition, for each system analyzed one must check if the system meets the acceleration requirements and if the configuration is capable of continuously producing any combination of force and speed in the operating range of the vehicle.

The results obtained are combined to a value function, the basic term of which is the calculated energy consumption, whereto are added terms for weight and volume, converted to increase of energy consumption as described earlier.

To the value function must also be added, for formal reasons, "penalty terms" for the cases where the acceleration and force continuity requirements are not fulfilled. These terms must, however, become zero when the value function is mini- mized, which means that at optimum conditions the acceleration requirements and driving force continuity are fulfilled.

## 9. METHODS OF EVALUATION

Numerical calculations have been carried out on an IBM computer, using the FORTRAN IV programming language.

The total computer program consists of a number of independent subroutines. The main subroutine blocks

- analyze the driving cycle and compile the matrix of the length of the driving time at various combinations of F and v (the driving cycle matrix)

- calculate the power consumed by each modeled component, provided that the operating conditions are known

- calculate the volume and weight of each modeled component

- check the acceleration and driving force continuity requirements

- find the operating conditions for a given set of components (maximum displacements and gear ratios) and boundary conditions (differential and back pressure, output force, and speed). This subroutine produces the data for the following system characteristics matrices: power loss, input flow, volumetric and total efficiencies, and control data (high/ low gear and yoke angle).
  In order to eliminate time-consuming iteration, the computation is based on a function-mapping technique, whereby F and v are mapped as dependent variables, being functions of input pressures and flow as well as of control data. Interpolation then gives flow and control data as functions of F and v

- find the optimized set of components characterized by the minimum point of the value function as defined in the preceding section. The direct search method, developed by Nealder & Mead, using the simplex concept for non-linear problems, has been used to avoid just trial and error techniques for the optimization *)

- prepare output data (interpolate data for drawing of performance maps, etc).

*) Elmén, Claes: Optimization of Hydraulic Transmission of Vehicle, M.Sc. thesis (in Swedish), Chalmers Univ. of Technology, Dept. of Mechanical Engineering (Machine Elements), 1980.

The computation is governed by a control program, calling on the various subroutines. Each computation requests the specification to the control program of input pressures (differential and back) and an assumed set of values of parameters to be optimized. The optimization algorithm guarantees only the detection of local minima; therefore various starting sets of parameter values must be tried to find the global minimum of the value function.

Found global minima are all very flat. Therefore, the optimization is not very distinct.

The results of each computation are obtained as definite values of the total energy loss and characteristics of optimized components: displacement/gear ratio, weight, and volume. In addition, system characteristics matrices are obtained as discrete data with increments in accordance with Fig. 4, and as computer-drawn constant-value graphs.

## 10. NUMERICAL RESULTS

The computer program package  developed in accordance with the
description in the preceding sections has been used to
analyze and optimize the hydrostatic drive systems A and B,
as defined in Figs. 14 and 15.

Both systems have been evaluated for 5 different differential
pressures:  6.895, 13.79, 20.68, 27.58, and 34.47 MPa (1000, 2000, 3000,
4000, and 5000 psi) and a negligible back pressure.

In addition, System A has been evaluated for 3 different back
pressures: 3.447, 6.895, and 13.79 MPa (500, 1000, and 2000 psi) at a
differential pressure of 20.68 MPa (3000 psi).

Optimized parameters are
for_System_A:

| | | |
|---|---|---|
| $D_{var}$ | = | displacement of the variable motor |
| $R_{low}$ | = | transmission ratio of the lower gear of the two-speed planetary gear train |
| $R'$ | = | transmission ratio of the final gear (in radians of revolution per traveled distance) |

for_System_B:

| | | |
|---|---|---|
| $D_{var}$ | = | displacement of the variable machine |
| $D_{fix}$ | = | displacement of the fixed motor |
| $R_{conn}$ | = | transmission ratio of the connecting gear |
| $R'$ | = | transmission ratio of the final gear (in radians of revolution per traveled distance) |

Calculated quantitites for each set of optimized parameters are:

| | | |
|---|---|---|
| $E_{loss}$ | = | energy loss during completion of the EPA Urban Driving Cycle |
| We | = | package weight |
| Vo | = | package volume |

The theoretical amount of energy required to complete the EPA
Urban Driving Cycle is the same for all cases evaluated:

$$E_{theor} = 6.70 * 10^6 \text{ Nm} \tag{71}$$

The above-mentioned optimized and evaluated data is given in Table 4.

In addition to the limited amount of summarized information given in Table 4, a large amount of detailed data has been calculated for each of the 13 cases evaluated.

For each case, data of the following performance characteristics matrices has been evaluated:

- total efficiency
- volumetric efficiency
- control data ( $\epsilon$ and high/low gear)
- power loss
- input flow rate

Each matrix contains about 5500 non-zero combinations of speed and force with a speed increment of 0.5 m/s and a force increment of 50 N. This number of data has been used to prepare the performance maps given in Appendix 3. The results obtained are illustrated by the reduced size performance maps depicted in Figs. 20 through 24 , computed for System A at a 20.68 MPa differential pressure and negligible back pressure.

The computed performance data points are also stored as data files on computer recording tape. The stored amount of data has been reduced by deleting every second row and column of the original performance characteristics matrices.

46

TABLE 4. Principal computed results for systems A and B

(The weight We and volume Vo include the following components: the variable machine and the train or the fixed machine, the connecting drive and the clutch, alternatively)

| System | $\Delta P$ MPa | $P_{back}$ MPa | $D_{var}$ $10^{-6}$ m$^3$ | $D_{Fix}$ $10^{-6}$ m$^3$ | $R_{low}$ | $R_{conn}$ | $R'$ 1/m | $E_{loss}$ $10^6$ Nm | We kg | Vo $10^{-3}$ m$^3$ |
|---|---|---|---|---|---|---|---|---|---|---|
| A | 34.47 | negl. | 96,0 | – | 2.98 | – | 3.22 | 4.96 | 95.2 | 47.2 |
| | 26.58 | " | 112 | – | 2.91 | – | 3.56 | 4.68 | 106 | 54.3 |
| | 20.68 | " | 142 | – | 2.99 | – | 3.67 | 4.48 | 127 | 67.0 |
| | 13.79 | " | 255 | – | 2.72 | – | 3.37 | 4.42 | 215 | 119 |
| | 6.895 | " | 473 | – | 3.35 | – | 3.05 | 4.51 | 377 | 217 |
| | 20.68 | " | 142 | – | 2.99 | – | 3.67 | 4.48 | 127 | 67.0 |
| | " | 3.447 | 141 | – | 2.98 | – | 3.71 | 4.88 | 130 | 70.7 |
| | " | 6.895 | 141 | – | 2.99 | – | 3.68 | 5.31 | 130 | 70.5 |
| | " | 13.79 | 141 | – | 2.99 | – | 3.69 | 6.35 | 130 | 70.5 |
| B | 34.47 | negl. | 96.0 | 64.9 | – | 2.46 | 3.59 | 5.64 | 113 | 62.2 |
| | 26.58 | " | 124 | 78.0 | – | 2.61 | 3.53 | 5.43 | 140 | 77.0 |
| | 20.68 | " | 155 | 114 | – | 1.67 | 4.43 | 5.06 | 179 | 97.0 |
| | 13.79 | " | 211 | 154 | – | 1.89 | 4.62 | 4.97 | 241 | 129 |
| | 6.89 | " | 393 | 314 | – | 1.58 | 5.30 | 5.20 | 452 | 238 |
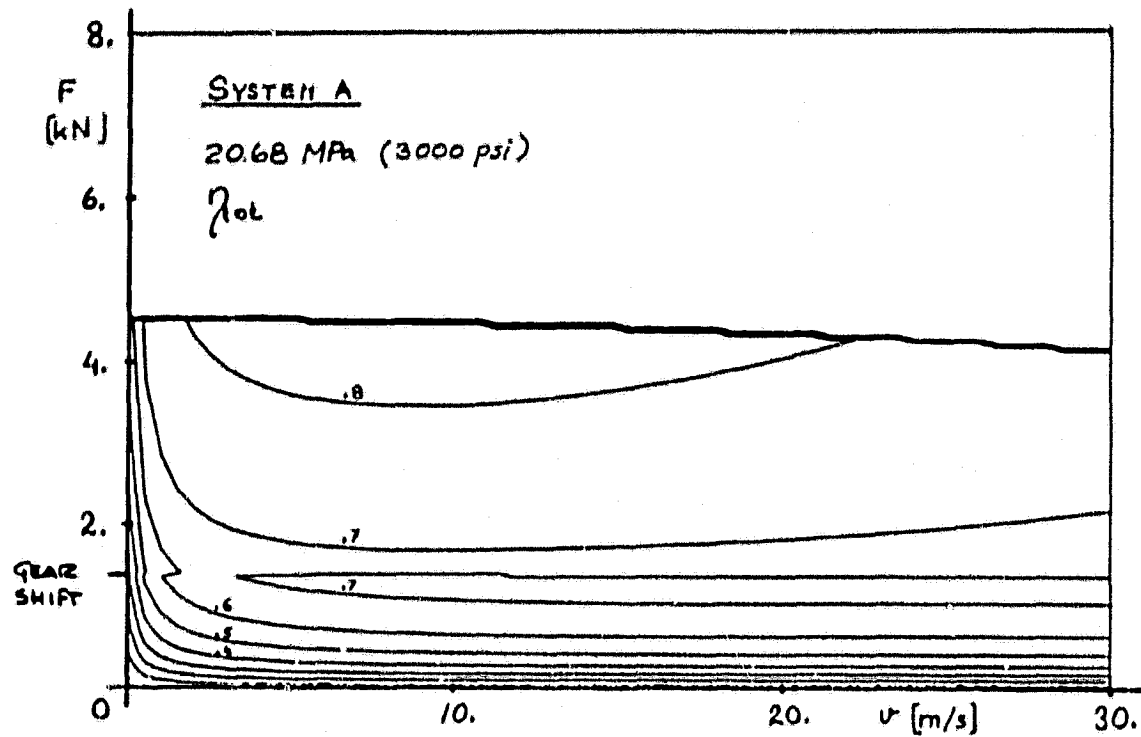
Fig. 20. Performance map = total efficiency
(complete drive system)
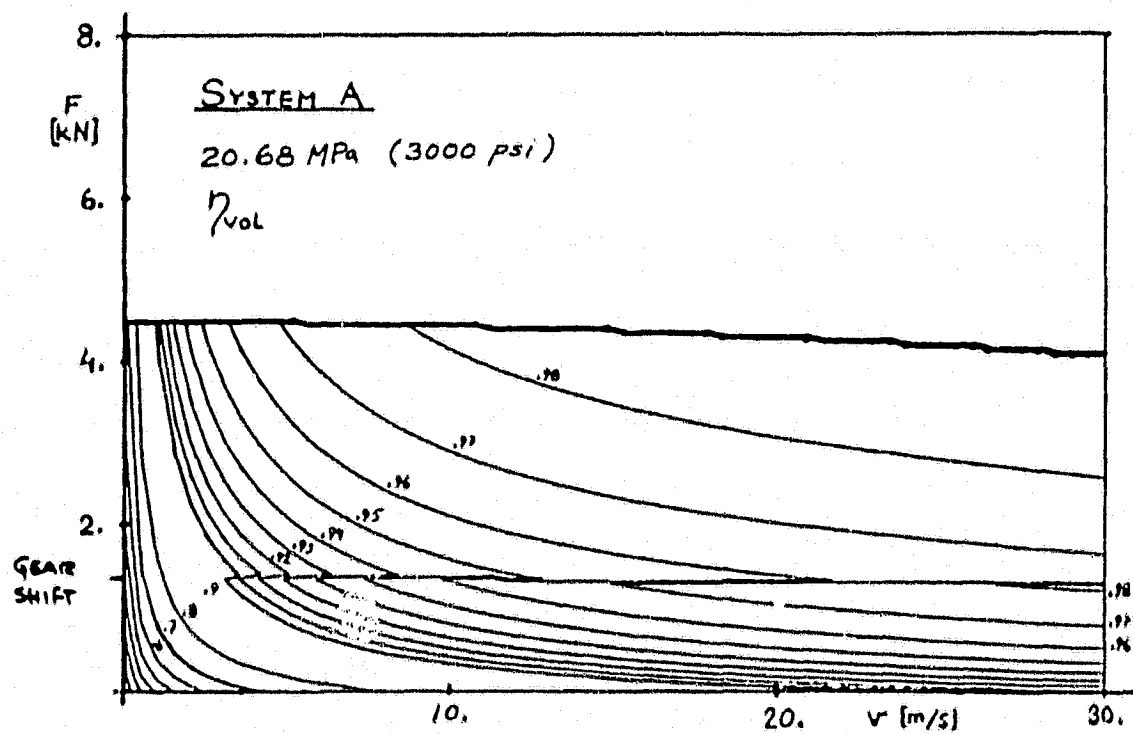


Fig. 21. Performance map - volumetric efficiency
(hydrostatic unit)

48
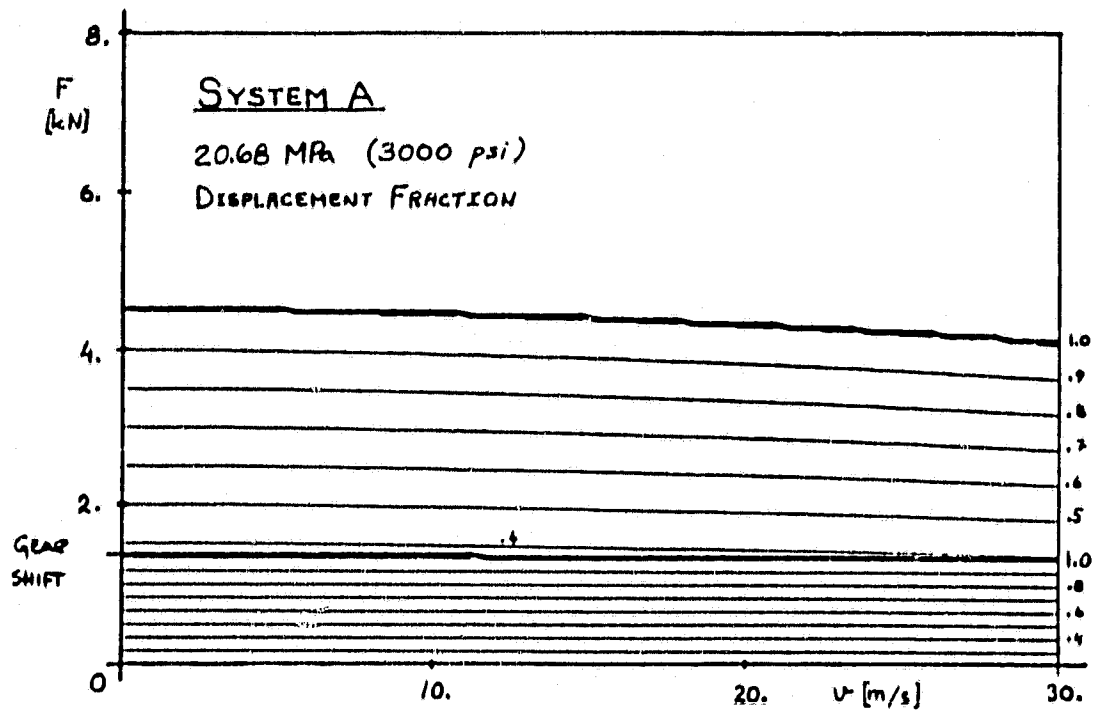


Fig. 22. Performance map - control data
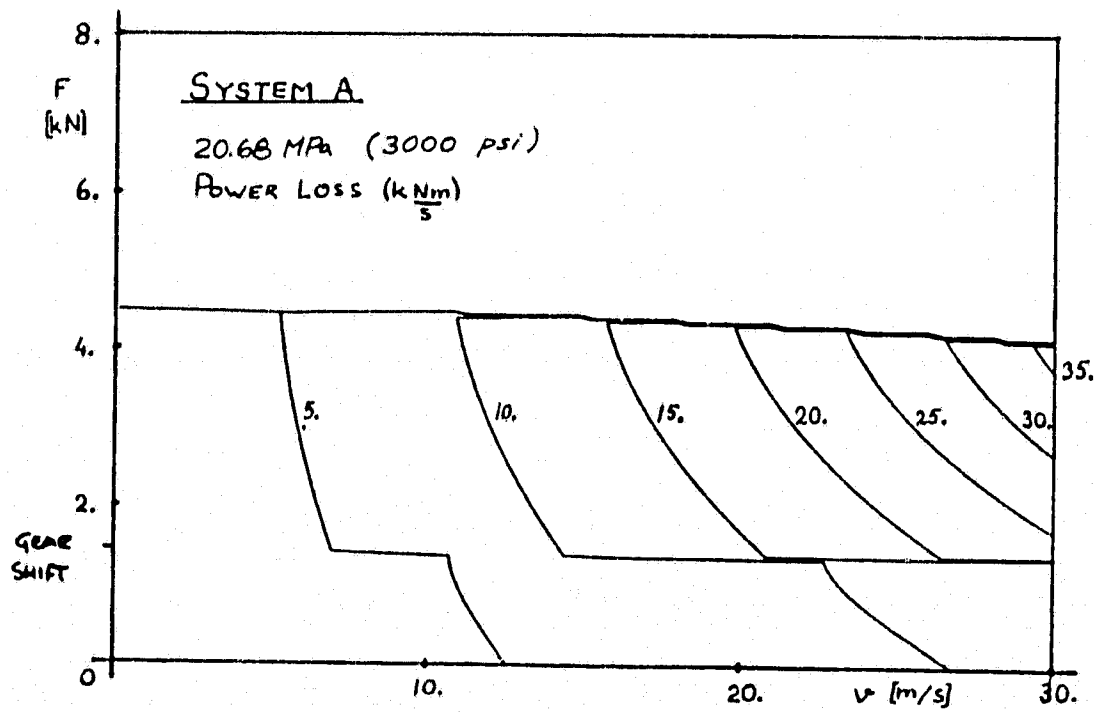


Fig. 23. Performance map - power loss
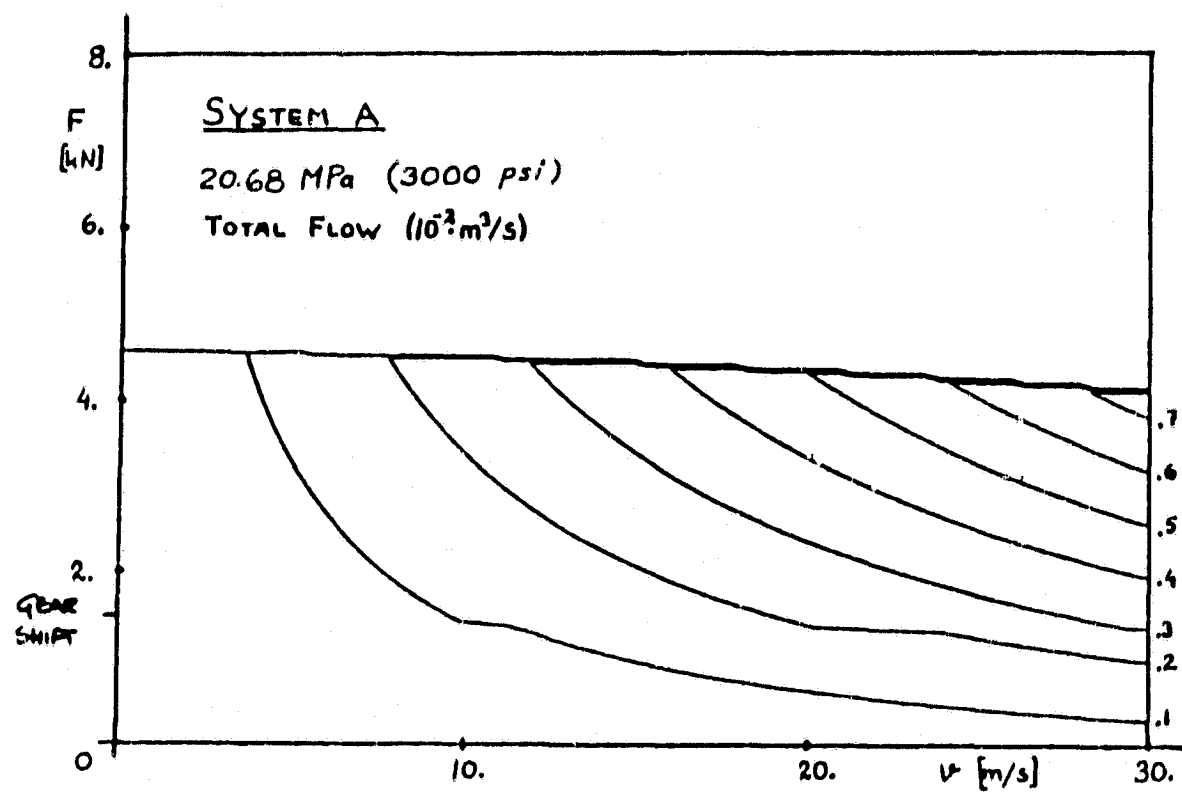
Fig. 24. Performance map - input flow rate

## 11. CONCLUDING REMARKS

### Limitations in Theory Used

1. The theoretical model assumes perfect external control of torque, and no time losses are considered when applying the initial torque and when shifting the gears.

2. The influence of secondary units, e.g., valves, filters, and hoses, is not considered when calculating losses and evaluating package weight and volume. (The influence is assumed to be the same for all cases studied).

### Component Models

3. The model of the VFA V20-180 machine predicts - in the loaded regime - loss values that are very close to the only set of available experimental results, but are somewhat lower (i.e. higher efficiency) than the values from the accumulated experience from V20-135 machines. The state-of-the-art of loss modeling does not permit an excellent loss prediction in the low-load regime of hydraulic machinery.

4. The model of the F-11 machines seems to overestimate the efficiency by maximum 2% in the high-load regime.

5. The loss models of the mechanical components are deliverately designed to be somewhat conservative. The real efficiencies of these components might be improved by a few percent.

6. The modeling of weight and volume of mechanical geared components depends very much on the assumptions made. Therefore, given data are to be considered more as an educated guess than definite values.

### Obtained Results

7. All calculated optima are rather indistinct, i.e. neighbouring parameter values give almost the same performance characteristics.

8. The total losses are almost independent of pressures used; however, the weights and volumes of the systems increase drastically at decreasing differential pressure.

9. Calculated energy losses may be converted to milage figures for the EPA Driving Cycle. Assuming a 30% engine efficiency and a 95% efficiency of an additional hydrostatic pump connected to the engine, the best cases investigated will have a fuel (gasoline) consumption of less than 10 liters per 100 kilometer (23.7 mpg).

10. Obtained control strategies deviate somewhat from initial assumptions resulting in slightly "oversized" hydraulic components. This is especially true for system B, were power recirculation (PRC) tends to be suppressed.

52

Appendix 1:      Configurations of Candidate Systems

## DESCRIPTION OF CANDIDATE SYSTEMS

In the following description of candidate systems only
the main components have been listed, as e.g. the hydro-
static motors, and necessary clutches and gears.
Hydraulic valves and the (microprocessor-based) control
system, as well as the final transmission have been
excluded. As we do not manufacture hydraulic valves to
be used outside our units the background for predicting
the development on those parts is limited to some extent.

$D_{1,2}...$ indicate maximum (or constant) displacement of
the hydrostatic machines, $\varepsilon$ indicates the fraction of
the max displacement used.

F indicates the driving force

$P_1/P_2$ indicate the hydrostatic supply and back pressure

$C_{1,2}...$ indicate clutches

$G_{1,2}...$ indicate single-step gear transmissions

# 1. Single motor

hydraulic
power input

mechanical
power output

D$_1$



F

theor., η=1

real (qualitati-
vely), η<1

0                                    1        c
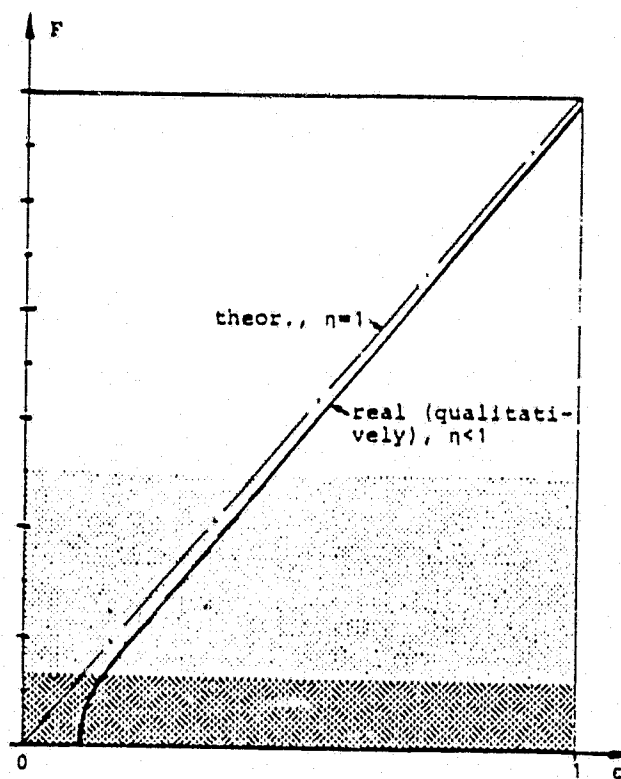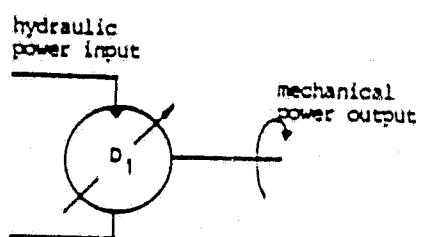
## 2. Two Motors, Clutched in Parallel to an Ordinary Shaft.

### 2a Two variable motors



$D_2 \sim 2.5D_1$, gear ratio 1
$C_1$ or $C_2$ in operation
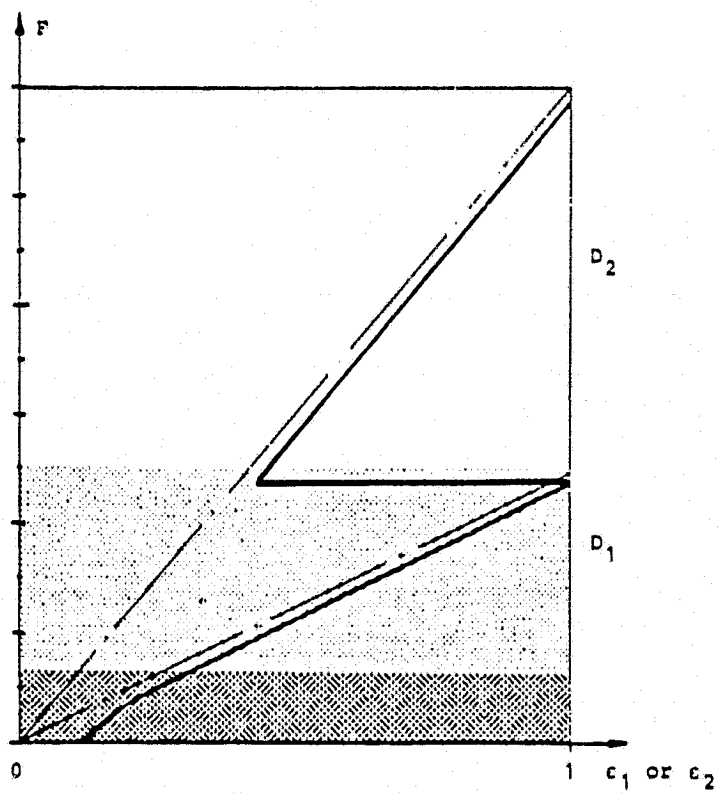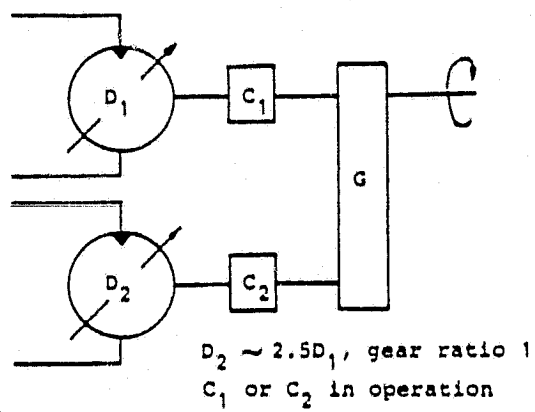
## 2b  Two variable motors as in 2a
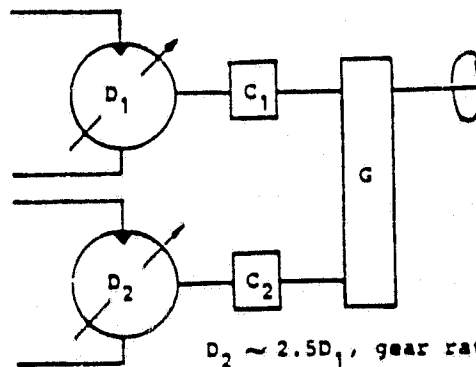


$D_2 \sim 2.5 D_1$, gear ratio 1
$C_1$ and/or $C_2$ in operation
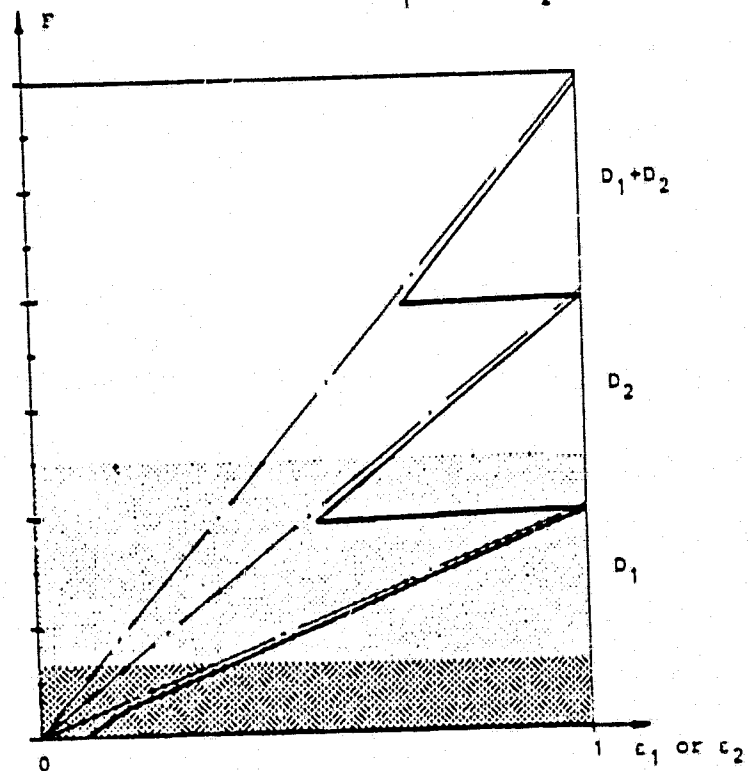
## 2c One variable and one fixed motor



$D_1 \sim D_2$, gear ratio 1

58
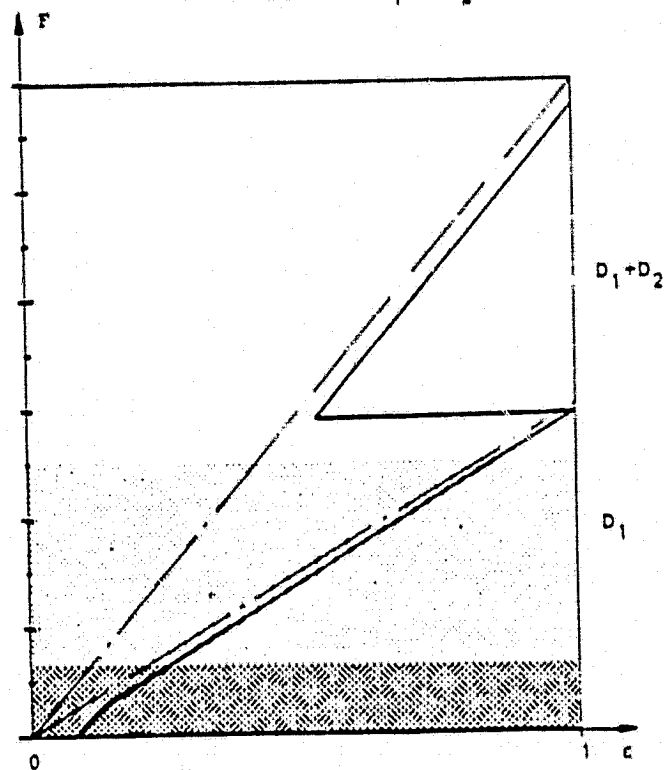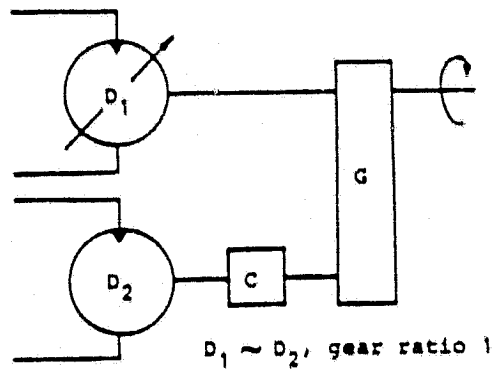
## 2d One variable and one fixed motor as 2c

In addition to the above configuration we use the "hydraulic polarity shift" for the $D_1$ unit in the higher force region where it partly operates as pump implying power circulation.



$2 D_1 \sim D_2$, gear ratio 1
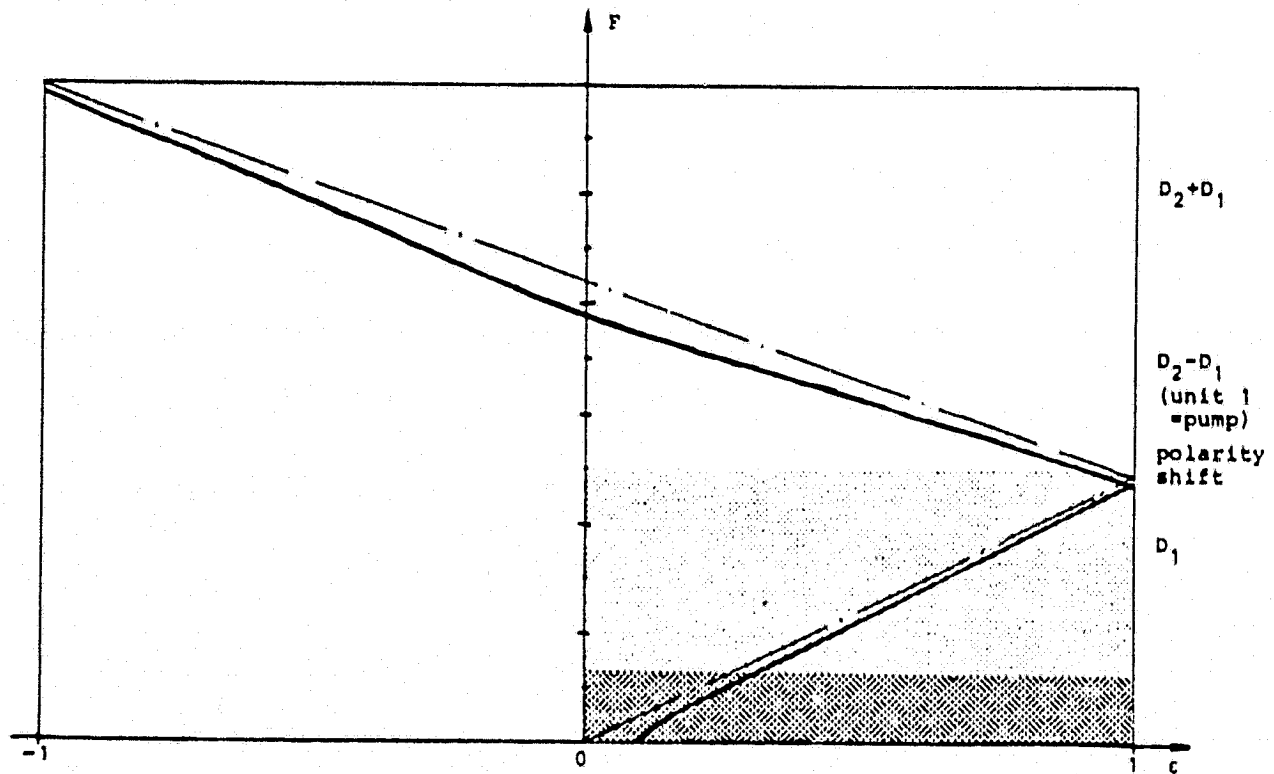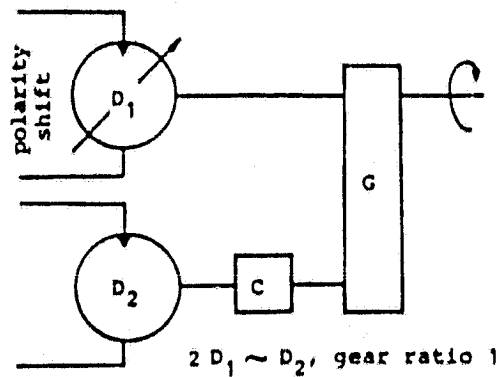
## 2e One variable and one fixed motor as 2c

Addition of "slow" hydraulic polarity swift for
unit $D_2$.



$D_1 \sim 2D_2$, gear ratio 1

## 3. One Single Motor With a Two Speed Transmission

# 4. Other Systems of Some Merit.

## 4a One single motor with a three speed transmission

Possible gear ratios   low       1:4

                          medium  1:2
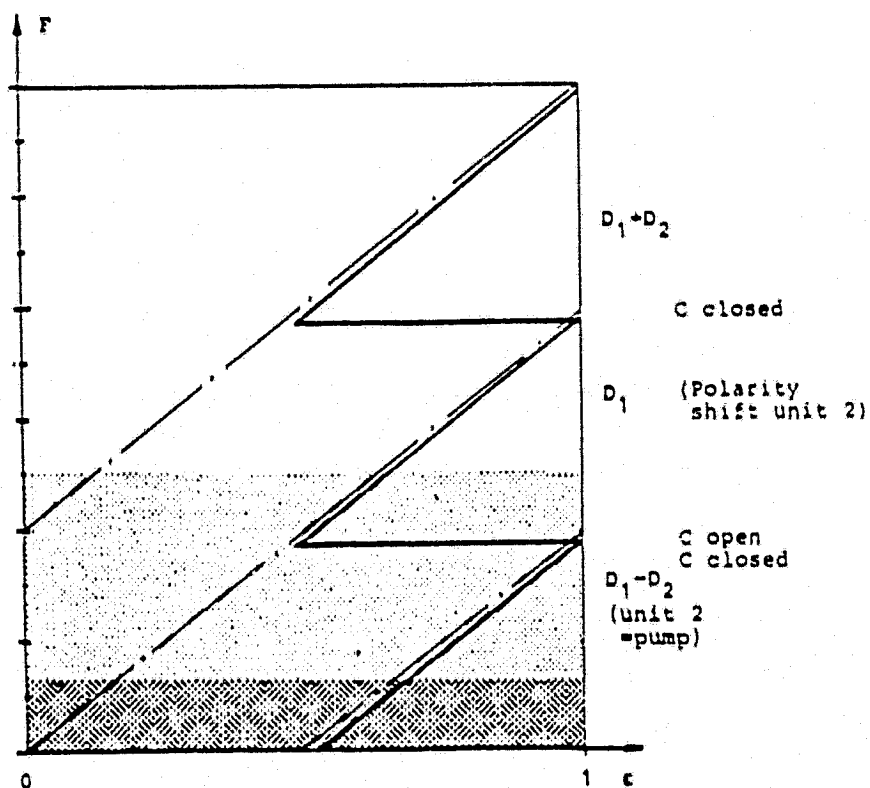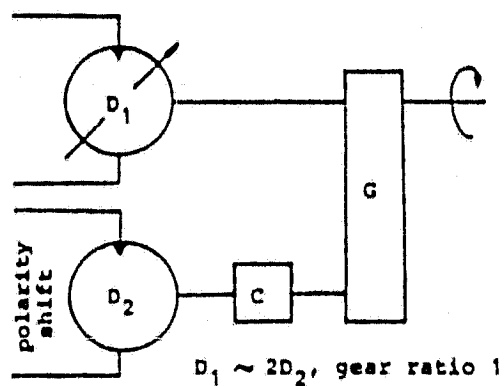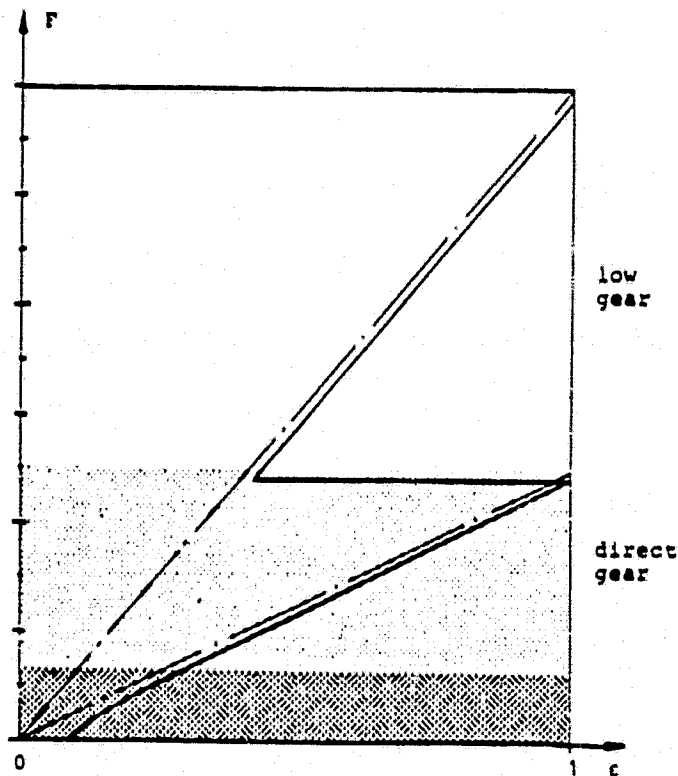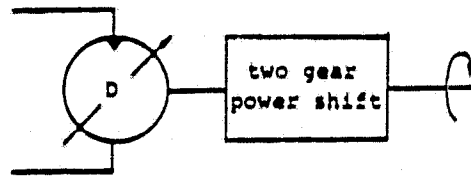
## 4b Two motors with a two speed transmission

Many choices of gear ratios are possible.



$D_2 \sim 2D_1$, $G_1 = 1:2$, $G_2 = 2:1$
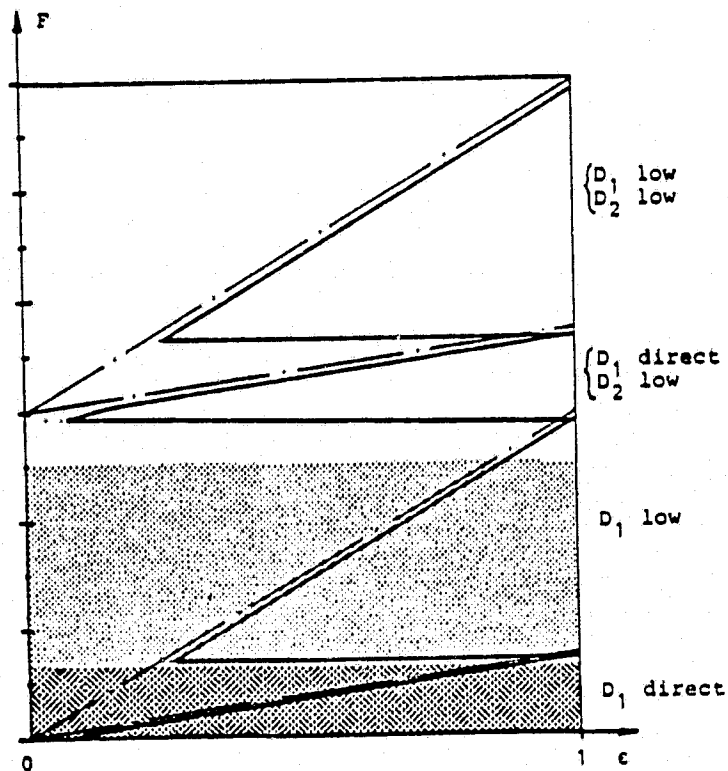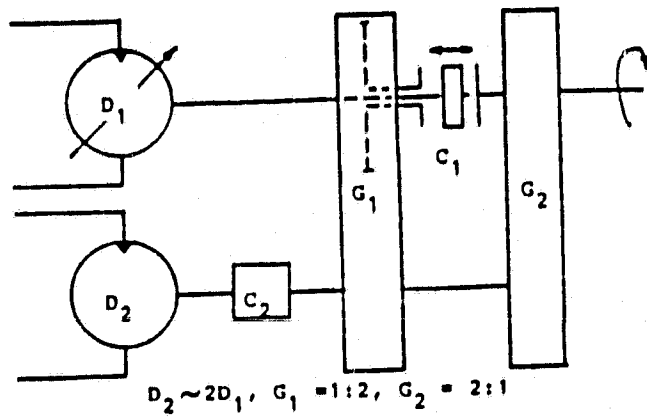
## 4c Three motors clutched in parallel without power circulation



$D_2 \sim D_1$, $D_3 \sim 2D_1$, gear ratio 1
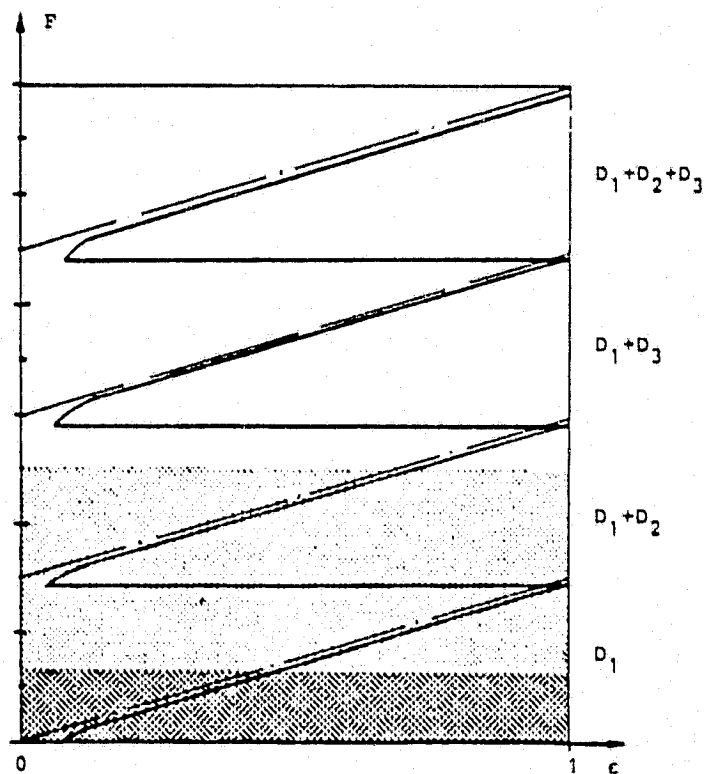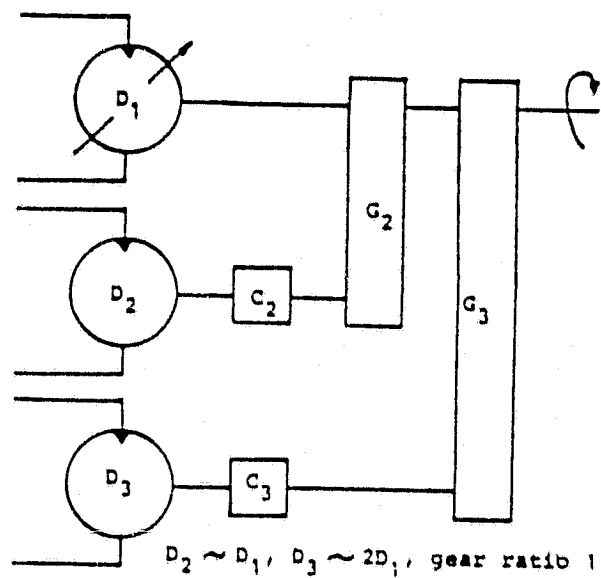
## 4d Three motors clutched in parallel with power circulation in the variable unit.

Arrangement same as 4c but with addition of possibility to change hydraulic polarity for unit D.



$D_2 \sim 2D_1$, $D_3 \sim 4D_1$, gear ratio 1
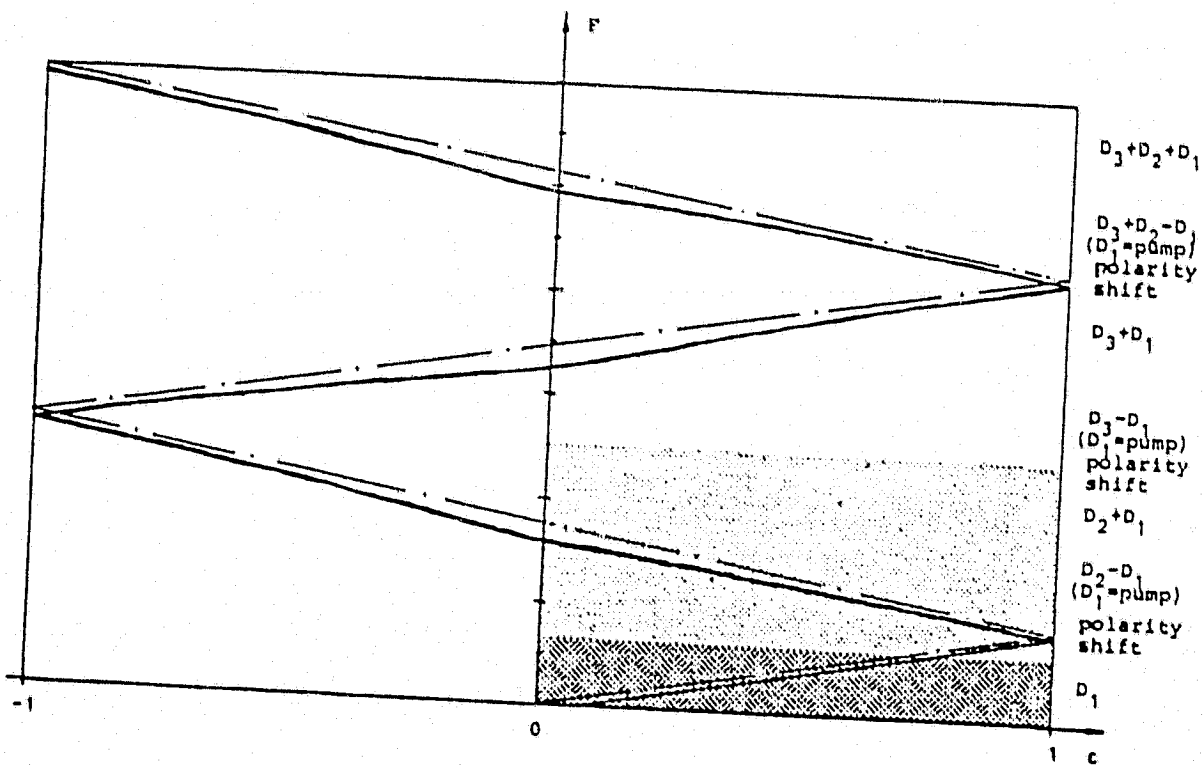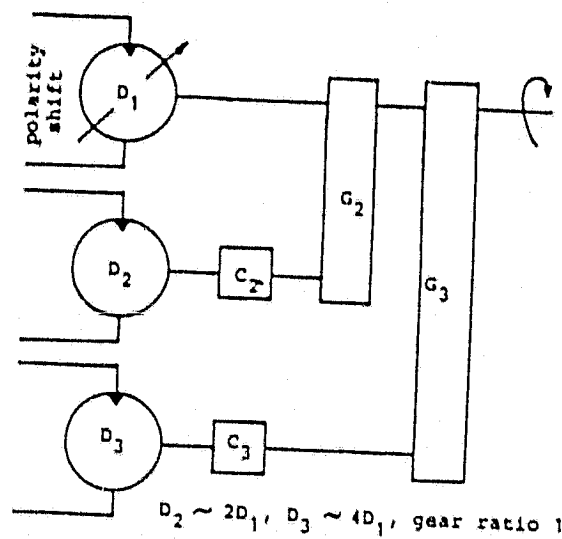
Appendix 2:    Test results V20-180 Machine

# V20-180 MACHINE

# OPERATING AS A PUMP

EFFICIENCY V20A-180
AS PUMP. OIL SHELL TELLUS 46. TEMP 50°C FEED PRESSURE 10 BAR

| DIFF. PRESSURE | | $\alpha = 40°$ SPEED RPM D= 178,07 cm$^3$/ Rev. | | | | |
|---|---|---|---|---|---|---|
| $\Delta$ p bar | | 500. | 1500 | 2000 | 2500 | 3000 |
| 0 | Vol. eff. | 0,998 | 0.999 | | | |
| | Mech. eff. | 0,000 | 0,000 | | | |
| | Tot. eff. | 0,000 | 0,000 | | | |
| 50 | | 0,988 | 0,995 | 0,996 | 0,995 | 0,995[x] |
| | | 0,920 | 0,854 | 0,824 | 0,785 | 0,738 |
| | | 0,909 | 0,850 | 0,821 | 0,781 | 0,734 |
| 150 | | 0,974 | 0,986 | 0,988 | 0,986 | 0,985[x] |
| | | 0,969 | 0,945 | 0,932 | 0,919 | 0,894 |
| | | 0,944 | 0,932 | 0,921 | 0,906 | 0,880 |
| 250 | | 0,956 | 0,975 | 0,978 | 0,977 | 0,976[x] |
| | | 0,982 | 0,968 | 0,956 | 0,947 | 0,936 |
| | | 0,939 | 0,944 | 0,935 | 0,925 | 0,914 |
| 350 | | 0,933 | 0,961 | 0,966 | 0,967 | 0,971[x] |
| | | 0,977 | 0,976 | 0,972 | 0,964 | 0,949 |
| | | 0,911 | 0,938 | 0,940 | 0,933 | 0,921 |

| | | $\alpha = 25°$ | | | D = 116,68 cm$^3$/ Rev. | |
|---|---|---|---|---|---|---|
| 0 | | 0,997 | 0,993 | 0,991 | 0,988 | |
| | | 0,000 | 0,000 | 0,000 | 0,000 | |
| | | 0,000 | 0,000 | 0,000 | 0,000 | |
| 50 | | 0,981 | 0,993 | 0,990 | 0,982 | 0,989 |
| | | 0,912 | 0,836 | 0,807 | 0,774 | 0,725 |
| | | 0,895 | 0,831 | 0,800 | 0,760 | 0,717 |
| 150 | | 0,972 | 0,974 | 0,974 | 0,972 | 0,977 |
| | | 0,947 | 0,935 | 0,929 | 0,913 | 0,893 |
| | | 0,921 | 0,910 | 0,904 | 0,888 | 0,872 |
| 250 | | 0,942 | 0,962 | 0,966 | 0,968 | 0,964 |
| | | 0,960 | 0,956 | 0,951 | 0,942 | 0,936 |
| | | 0,904 | 0,920 | 0,919 | 0,911 | 0,902 |
| 350 | | 0,902 | 0,943 | 0,950 | 0,953 | 0,951 |
| | | 0,956 | 0,960 | 0,959 | 0,957 | 0,953 |
| | | 0,863 | 0,906 | 0,911 | 0,912 | 0,907 |

x - Test data fell beyond the calibrated range of the
flowmeter. The number shown was calculated using
extrapolation.

| DIFF. PRESSURE | $\alpha = 15°$ SPEED RPM | | | | $D = 71,35 \text{ cm}^3/\text{Rev.}$ |
|---|---|---|---|---|---|
| $\Delta$ p bar | 500 | 1500 | 2000 | 2500 | 3000 |
| 0 Vol. eff. Mech.eff. Tot.eff. | 0,994 0,000 0,000 | 0,999 0,000 0,000 | 0,996 0,000 0,000 | | |
| 50 | 0.969 0,848 0,822 | 0,987 0,778 0,768 | 0,984 0,757 0,746 | 0,985 0,738 0,726 | 0,983 0,693 0,681 |
| 150 | 0,938 0,931 0,873 | 0,966 0,902 0,871 | 0,968 0,897 0,868 | 0,968 0,878 0,851 | 0,965 0,869 0,839 |
| 250 | 0,898 0,947 0,850 | 0,942 0,937 0,883 | 0,946 0,928 0,878 | 0,948 0,925 0,877 | 0,946 0,922 0,873 |
| 350 | | 0,914 0,946 0,865 | 0,920 0,942 0,867 | 0,924 0,938 0,866 | 0,924 0,943 0,872 |

| | $\alpha = 10°$ | | | | $D = 48,43 \text{ cm}^3/\text{Rev.}$ |
|---|---|---|---|---|---|
| 0 | 0,992 0,000 0,000 | 0,999 0,000 0,000 | 0,998 0,000 0,000 | 0,997 0,000 0,000 | 0,994 0,000 0,000 |
| 50 | 0,954 0,803 0,766 | 0,983 0,727 0,715 | 0,984 0,701 0,689 | 0,983 0,665 0,653 | 0,981 0,643 0,630 |
| 150 | 0,910 0,904 0,822 | 0,956 0,870 0,832 | 0,958 0,857 0,821 | 0,959 0,838 0,804 | 0,956 0,850 0,813 |
| 250 | 0,869 0,922 0,801 | 0,921 0,909 0,837 | 0,925 0,905 0,837 | 0,929 0,897 0,833 | 0,930 0,888 0,826 |
| 350 | | 0,877 0,924 0,810 | 0,886 0,924 0,819 | 0,893 0,921 0,823 | 0,893 0,918 0,820 |

| DIFF. PRESSURE | | $\alpha = 6°$  SPEED RPM | | | $D = 29{,}40\ \text{cm}^3/\text{Rev.}$ | |
|---|---|---|---|---|---|---|
| $\Delta p$ bar | | 500 | 1500 | 2000 | 2500 | 3000 |
| 0 | Vol. eff. | 0,993 | 0,999 | 0,999 | 0,999 | 0,999 |
|   | Mech. eff. | 0,000 | 0,000 | 0,000 | 0,000 | 0,000 |
|   | Tot. eff. | 0,000 | 0,000 | 0,000 | 0,000 | 0,000 |
| 50 |  | 0,931 | 0,972 | 0,975 | 0,978 | 0,977 |
|   |  | 0,709 | 0,632 | 0,585 | 0,557 | 0,532 |
|   |  | 0,660 | 0,614 | 0,570 | 0,545 | 0,519 |
| 150 |  | 0,864 | 0,928 | 0,931 | 0,937 | 0,939 |
|   |  | 0,856 | 0,816 | 0,789 | 0,771 | 0,755 |
|   |  | 0,739 | 0,757 | 0,734 | 0,732 | 0,709 |
| 250 |  |  | 0,872 | 0,881 | 0,891 | 0,895 |
|   |  |  | 0,873 | 0,854 | 0,848 | 0,842 |
|   |  |  | 0,761 | 0,752 | 0,755 | 0,753 |
| 350 |  |  | 0,811 | 0,828 | 0,840 | 0,847 |
|   |  |  | 0,895 | 0,886 | 0,879 | 0,869 |
|   |  |  | 0,726 | 0,734 | 0,738 | 0,736 |

| $\alpha = 3°$ | | | | | $D = 14{,}55\ \text{cm}^3/\text{Rev.}$ | |
|---|---|---|---|---|---|---|
| 0 |  |  | 0,999 | 0,999 | 0,999 | 0,999 |
|   |  |  | 0,000 | 0,000 | 0,000 | 0,000 |
|   |  |  | 0,000 | 0,000 | 0,000 | 0,000 |
| 50 |  |  | 0,943 | 0,954 | 0,957 | 0,956 |
|   |  |  | 0,464 | 0,430 | 0,400 | 0,374 |
|   |  |  | 0,437 | 0,410 | 0,383 | 0,358 |
| 150 |  |  | 0,854 | 0,867 | 0,878 | 0,883 |
|   |  |  | 0,696 | 0,669 | 0,633 | 0,621 |
|   |  |  | 0,594 | 0,580 | 0,556 | 0,549 |
| 250 |  |  | 0,749 | 0,767 | 0,796 | 0,800 |
|   |  |  | 0,784 | 0,763 | 0,744 | 0,725 |
|   |  |  | 0,587 | 0,585 | 0,592 | 0,580 |
| 350 |  |  | 0,621 | 0,658 | 0,679 | 0,697 |
|   |  |  | 0,823 | 0,806 | 0,796 | 0,787 |
|   |  |  | 0,511 | 0,530 | 0,540 | 0,549 |

# V20-180 MACHINE

# OPERATING AS A MOTOR

EFFICIENCY V20A-180
AS MOTOR. OIL SHELL TELLUS 46. TEMP 50°C BACK PRESSURE 10 BAR

| DIFF. PRESSURE | $\alpha = 40°$ SPEED RPM $D = 177,46$ cm³/ Rev. | | | | | | |
|---|---|---|---|---|---|---|---|
| Δp bar | 500 | 1500 | 2000 | 2500 | 3000 | 100 | 200 |
| 0    Vol. eff. | 0,999 | 0,999 | 0,998 | 0,998 | 0,999[x] | 0,995 | 0,996 |
|      Mech. eff. | 0,000 | 0,000 | 0,000 | 0,000 | 0,000 | 0,000 | 0,000 |
|      Tot. eff. | 0,000 | 0,000 | 0,000 | 0,000 | 0,000 | 0,000 | 0,000 |
| 50 | 0,992 | 0,995 | 0,995 | 0,996 | 0,996[x] | 0,952 | 0,976 |
|  | 0,934 | 0,849 | 0,793 | 0,729 | 0,651 | 0,948 | 0,970 |
|  | 0,926 | 0,845 | 0,789 | 0,726 | 0,649 | 0,903 | 0,946 |
| 150 | 0,981 | 0,990 | 0,990 | 0,991 | 0,992[x] |  | 0,955 |
|  | 0,977 | 0,953 | 0,925 | 0,906 | 0,882 |  | 0,984 |
|  | 0,958 | 0,943 | 0,916 | 0,898 | 0,875 |  | 0,939 |
| 250 | 0,967 | 0,982 | 0,984 | 0,985 | 0,986[x] |  |  |
|  | 0,981 | 0,964 | 0,950 | 0,936 | 0,923 |  |  |
|  | 0,948 | 0,947 | 0,935 | 0,922 | 0,910 |  |  |
| 350 | 0,947 | 0,974 | 0,978 | 0,980 | 0,982[x] |  |  |
|  | 0,982 | 0,974 | 0,962 | 0,949 | 0,938 |  |  |
|  | 0,930 | 0,949 | 0,940 | 0,929 | 0,921 |  |  |

| $\alpha = 25°$ | | | | $D = 114,48$ cm³/ Rev. | | | |
|---|---|---|---|---|---|---|---|
| 0 | 0,994 | 0,999 | 0,993 | 0,991 | 0,996 | 0,999 | 0,967 |
|  | 0,000 | 0,000 | 0,000 | 0,000 | 0,000 | 0,000 | 0,000 |
|  | 0,000 | 0,000 | 0,000 | 0,000 | 0,000 | 0,000 | 0,000 |
| 50 | 0,982 | 0,996 | 0,968 | 0,967 | 0,993 | 0,940 | 0,956 |
|  | 0,944 | 0,845 | 0,801 | 0,735 | 0,659 | 0,911 | 0,944 |
|  | 0,927 | 0,841 | 0,792 | 0,726 | 0,654 | 0,856 | 0,902 |
| 150 | 0,968 | 0,986 | 0,981 | 0,980 | 0,986 |  | 0,924 |
|  | 0,970 | 0,940 | 0,933 | 0,911 | 0,882 |  | 0,970 |
|  | 0,939 | 0,928 | 0,915 | 0,893 | 0,870 |  | 0,896 |
| 250 | 0,952 | 0,972 | 0,970 | 0,971 | 0,978 |  |  |
|  | 0,968 | 0,959 | 0,953 | 0,942 | 0,922 |  |  |
|  | 0,922 | 0,932 | 0,925 | 0,914 | 0,901 |  |  |
| 350 | 0,928 | 0,956 | 0,959 | 0,960 | 0,963 |  |  |
|  | 0,967 | 0,970 | 0,963 | 0,956 | 0,945 |  |  |
|  | 0,898 | 0,927 | 0,923 | 0,918 | 0,910 |  |  |

x - Test data fell beyond the calibrated range of the
    flowmeter. The number shown was calculated using
    extrapolation.

| DIFF. PRESSURE | $\alpha = 15°$ | SPEED RPM | | | | $D = 70,54 \ cm^3$/Rev. | |
|---|---|---|---|---|---|---|---|
| $\Delta p$ bar | 500 | 1500 | 2000 | 2500 | 3000 | 100 | 200 |
| 0   Vol.eff. <br> Mech. eff. <br> Tot. eff. | 0,991 <br> 0,000 <br> 0,000 | 0,999 <br> 0,000 <br> 0,000 | 0,995 <br> 0,000 <br> 0,000 | 0,991 <br> 0,000 <br> 0,000 | 0,987 <br> 0,000 <br> 0,000 | 0,999$^x$ <br> 0,000 <br> 0,000 | 0,982 <br> 0,000 <br> 0,000 |
| 50 | 0,969 <br> 0,890 <br> 0,863 | 0,991 <br> 0,784 <br> 0,771 | 0,988 <br> 0,730 <br> 0,721 | 0,984 <br> 0,677 <br> 0,666 | 0,980 <br> 0,623 <br> 0,611 | 0,897$^x$ <br> 0,855 <br> 0,767 | 0,930 <br> 0,908 <br> 0,845 |
| 150 | 0,943 <br> 0,950, <br> 0,895 | 0,976 <br> 0,920 <br> 0,898 | 0,974 <br> 0,902 <br> 0,879 | 0,971 <br> 0,890 <br> 0,865 | 0,968 <br> 0,873 <br> 0,845 | | 0,883 <br> 0,950 <br> 0,839 |
| 250 | 0,916 <br> 0,955 <br> 0,875 | 0,955 <br> 0,937 <br> 0,895 | 0,957 <br> 0,933 <br> 0,893 | 0,956 <br> 0,926 <br> 0,885 | 0,954 <br> 0,915 <br> 0,873 | | |
| 350 | 0,875 <br> 0,954 <br> 0,838 | 0,928 <br> 0,954 <br> 0,885 | 0,935 <br> 0,948 <br> 0,886 | 0,938 <br> 0,945 <br> 0,886 | 0,936 <br> 0,936 <br> 0,877 | | |

| | $\alpha = 10°$ | | | | | $D = 47,13 \ cm^3$/Rev. | |
|---|---|---|---|---|---|---|---|
| 0 | 0,991 <br> 0,000 <br> 0,000 | 0,999 <br> 0,000 <br> 0,000 | 0,989 <br> 0,000 <br> 0,000 | 0,990 <br> 0,000 <br> 0,000 | 0,989 <br> 0,000 <br> 0,000 | 0,999$^x$ <br> 0,000 <br> 0,000 | 0,999$^x$ <br> 0,000 <br> 0,000 |
| 50 | 0,956 <br> 0,853 <br> 0,816 | 0,984 <br> 0,693 <br> 0,682 | 0,976 <br> 0,640 <br> 0,625 | 0,977 <br> 0,560 <br> 0,547 | 0,977 <br> 0,507 <br> 0,495 | 0,817$^x$ <br> 0,827 <br> 0,675 | 0,918$^x$ <br> 0,880 <br> 0,807 |
| 150 | 0,917 <br> 0,942 <br> 0,864 | 0,961 <br> 0,889 <br> 0,854 | 0,955 <br> 0,871 <br> 0,832 | 0,958 <br> 0,853 <br> 0,817 | 0,957 <br> 0,827 <br> 0,791 | | 0,843$^x$ <br> 0,942 <br> 0,794 |
| 250 | 0,871 <br> 0,949 <br> 0,827 | 0,933 <br> 0,912 <br> 0,851 | 0,931 <br> 0,907 <br> 0,844 | 0,935 <br> 0,901 <br> 0,843 | 0,935 <br> 0,891 <br> 0,833 | | |
| 350 | 0,800 <br> 0,944 <br> 0,755 | 0,895 <br> 0,939 <br> 0,841 | 0,904 <br> 0,932 <br> 0,842 | 0,909 <br> 0,926 <br> 0,842 | 0,910 <br> 0,915 <br> 0,833 | | |

x - Test data fell beyond the calibrated range of the
flowmeter. The number shown was calculated using
extrapolation.

| DIFF. PRESSURE | $\alpha = 6^{\circ}$ | | SPEED RPM | | $D = 28,97 \ cm^3/$ Rev. | |
|---|---|---|---|---|---|---|
| $\Delta p$ bar | 500 | 1500 | 2000 | 2500 | 3000 | 200 |
| 0   Vol. eff.<br>    Mech. eff.<br>    Tot. eff. | 0,988<br>0,000<br>0,000 | 0,999<br>0,000<br>0,000 | 0,996<br>0,000<br>0,000 | 0,990<br>0,000<br>0,000 | 0,985<br>0,000<br>0,000 | 0,999[x]<br>0,000<br>0,000 |
| 50 | 0,932<br>0,738<br>0,688 | 0,976<br>0,521<br>0,508 | 0,974<br>0,434<br>0,423 | 0,971<br>0,347<br>0,337 | 0,968<br>0,260<br>0,252 | 0,859[x]<br>0,781<br>0,671 |
| 150 | 0,862<br>0,897<br>0,773 | 0,938<br>0,810<br>0,759 | 0,939<br>0,795<br>0,747 | 0,937<br>0,752<br>0,705 | 0,936<br>0,738<br>0,690 | 0,754[x]<br>0,897<br>0,676 |
| 250 | 0,706<br>0,920<br>0,649 | 0,894<br>0,868<br>0,776 | 0,900<br>0,859<br>0,773 | 0,902<br>0,850<br>0,767 | 0,898<br>0,842<br>0,756 | |
| 350 | | 0,843<br>0,907<br>0,765 | 0,851<br>0,901<br>0,767 | 0,859<br>0,892<br>0,767 | 0,858<br>0,890<br>0,763 | |

| | $\alpha = 4^{\circ}$ | | | | $D = 19,73 \ cm^3/$ Rev. | |
|---|---|---|---|---|---|---|
| 0 | 0,989[x]<br>0,000<br>0,000 | 0,997<br>0,000<br>0,000 | 0,998<br>0,000<br>0,000 | 0,999<br>0,000<br>0,000 | 0,998<br>0,000<br>0,000 | 0,999[x]<br>0,000<br>0,000 |
| 50 | 0,902[x]<br>0,637<br>0,575 | 0,958<br>0,318<br>0,305 | 0,965<br>0,191<br>0,184 | 0,973<br>0,064<br>0,062 | 0,967<br>0,000<br>0,000 | 0,694[x]<br>0,764<br>0,531 |
| 150 | 0,707[x]<br>0,849<br>0,601 | 0,903<br>0,743<br>0,671 | 0,914<br>0,701<br>0,640 | 0,924<br>0,658<br>0,608 | 0,919<br>0,616<br>0,566 | 0,534[x]<br>0,870<br>0,465 |
| 250 | | 0,844<br>0,828<br>0,699 | 0,860<br>0,803<br>0,690 | 0,871<br>0,777<br>0,677 | 0,866<br>0,752<br>0,651 | |
| 350 | | 0,779<br>0,864<br>0,673 | 0,803<br>0,846<br>0,680 | 0,813<br>0,828<br>0,673 | 0,805<br>0,832<br>0,670 | |

x - Test data fell beyond the calibrated range of the
flowmeter. The number shown was calculated using
extrapolation.

| DIFF. PRESSURE | $\alpha = 3°$ | | SPEED RPM | | $D = 14,74 \text{ cm}^3/\text{Rev.}$ | |
|---|---|---|---|---|---|---|
| $\Delta$ p bar | 500 | 1500 | 2000 | 2500 | 3000 | |
| 0  Vol. eff. | 0,999 | 0,998 | 0,999 | 0,999 | 0,999 | |
| Mech. eff. | 0.000 | 0,000 | 0,000 | 0,000 | 0,000 | |
| Tot. eff. | 0,000 | 0,000 | 0,000 | 0,000 | 0,000 | |
| 50 | 0.879 | 0,947 | 0,958 | 0,961 | 0,956 | |
| | 0,511 | 0,085 | 0,000 | 0,000 | 0,000 | |
| | 0,449 | 0,081 | 0,000 | 0,000 | 0,000 | |
| 150 | | 0,879 | 0,890 | 0,900 | 0,894 | |
| | | 0,652 | 0,596 | 0,539 | 0,462 | |
| | | 0,574 | 0,530 | 0,485 | 0,431 | |
| 250 | | 0,810 | 0,821 | 0,835 | 0,833 | |
| | | 0,766 | 0,732 | 0,715 | 0,664 | |
| | | 0,620 | 0,601 | 0,597 | 0,553 | |
| 350 | | 0,733 | 0,748 | 0,768 | 0,770 | |
| | | 0,827 | 0,802 | 0,778 | 0,754 | |
| | | 0,606 | 0,600 | 0,597 | 0,580 | |

# EFFECT OF ELEVATED TEMPERATURE

# ON V20-180 MACHINE

# OPERATING AS A MOTOR

MOTOR
TEMP. 70°C   VISCOSITY   16 cSt   BACK PRESSURE 10 BAR

| DIFF. PRESSURE | | $\alpha = 25°$ | | $= 10°$ | |
|---|---|---|---|---|---|
| $\Delta$ p bar | | 500 | 2500 | 500 | 2500 |
| 50 | Vol. eff. | 0,985 | 0,994 | 0,979 | 0,989 |
| | Mech. eff. | 0,933 | 0,744 | 0,868 | 0,605 |
| | Tot. eff. | 0,919 | 0,740 | 0,850 | 0,599 |
| 150 | | 0,963 | 0,985 | 0,925 | 0,965 |
| | | 0,959 | 0,907 | 0,939 | 0,860 |
| | | 0,924 | 0,894 | 0,868 | 0,829 |
| 250 | | 0,935 | 0,973 | 0,836 | 0,934 |
| | | 0,962 | 0,938 | 0,937 | 0,900 |
| | | 0,900 | 0,913 | 0,784 | 0,841 |
| 350 | | 0,902 | 0,960 | | 0,902 |
| | | 0,958 | 0,951 | | 0,921 |
| | | 0,864 | 0,913 | | 0,831 |

# EFFECT OF HIGH BACK

# PRESSURE ON V20-180 MACHINE

# OPERATING AS A MOTOR

MOTOR
TEMP 50°C   VISCOSITY  30 cSt   BACK PRESSURE 100 BAR

| DIFF. PRESSURE | $\alpha = 25°$ | | $= 10°$ | |
|---|---|---|---|---|
| $\Delta p$ bar | 500 | 2500 | 500 | 2500 |
| 50  Vol. eff. | 0,973 | 0,993 | 0,949 | 0,987 |
|      Mech. eff | 0,901 | 0,717 | 0,763 | 0,500 |
|      Tot. eff. | 0,877 | 0,712 | 0,724 | 0,493 |
| 150 | 0,954 | 0,985 | 0,898 | 0,964 |
|     | 0,934 | 0,887 | 0,877 | 0,798 |
|     | 0,891 | 0,873 | 0,787 | 0,770 |
| 250 | 0,935 | 0,974 | 0,853 | 0,941 |
|     | 0,940 | 0,893 | 0,895 | 0,868 |
|     | 0,879 | 0,869 | 0,764 | 0,818 |

## Appendix 3:    PERFORMANCE MAPS OF OPTIMIZED SYSTEMS

SYSTEMS A AND B
  Pressures 34.47, 27.58, 20.68, 13.79 and 6.895 MPa
  (5000, 4000, 3000, 2000 and 1000 psi)

SYSTEM A
  Differential pressure 20.68 MPa (3000 psi)
  Backpressures 3.447, 6.895, 13.79 MPa
  (500, 1000, 2000 psi)

VARIABLES
  Total efficiency
  Volymetric efficiency
  Displacement fraction
  Power loss
  Total flow

SYSTEM A
34.47 MPa (5000 psi)
$\eta_{tot}$



SYSTEM A
34.47 MPa (5000 psi)
$\eta_{vol}$

SYSTEM A
34.47 MPa (5000 psi)
POWER LOSS (kNm/s)



SYSTEM A
34.47 MPa (5000 psi)
DISPLACEMENT FRACTION

SYSTEM A

34.47 MPa (5000 psi)

TOTAL FLOW ($10^{-2}$ m³/s)



SYSTEM A

27.58 MPa (4000 psi)

$\eta_{tot}$

SYSTEM A

27.58 MPa (4000 psi)

1/vol



SYSTEM A

27.58 MPa (4000 psi)

POWER LOSS (k$\frac{Nm}{s}$)

SYSTEM A

27.58 MPa (4000 psi)

DISPLACEMENT FRACTION



SYSTEM A

27.58 MPa (4000 psi)

TOTAL FLOW ($10^{-2} m^3/s$)

SYSTEM A

20.68 MPa  (3000 psi)

$\eta_{ot}$

F [kN]

$v$ [m/s]



SYSTEM A

20.68 MPa  (3000 psi)

$\eta_{vol}$

F [kN]

$v$ [m/s]

SYSTEM A

20.68 MPa (3000 psi)

DISPLACEMENT FRACTION



SYSTEM A

20.68 MPa (3000 psi)

POWER LOSS (k$\frac{Nm}{s}$)

SYSTEM A

20.68 MPa (3000 psi)

TOTAL FLOW ($10^{-3}$ m³/s)



SYSTEM A

13.79 MPa (2000 psi)

$\eta_{tot}$

SYSTEM A

13.79 MPa  (2000 psi)

$\eta_{vol}$



SYSTEM A

13.79 MPa  (2000 psi)

DISPLACEMENT FRACTION

SYSTEM A.
13.79 MPa (2000 psi)
POWER LOSS (k Nm / S)



SYSTEM A
13.79 MPa (2000 psi)
TOTAL FLOW (10⁻² m³/s)

SYSTEM A

6.895 MPa (1000 psi)

$\eta_{tot}$



SYSTEM A

6.895 MPa (1000 psi)

$\eta_{vol}$

SYSTEM A

6.895 MPa (1000 psi)
DISPLACEMENT FRACTION



SYSTEM A

6.895 MPa (1000 psi)
POWER LOSS (k$\frac{Nm}{s}$)

SYSTEM A

6.895 MPa  (1000 psi)
TOTAL FLOW  ($10^{-2}$ m³/s)

SYSTEM B
34.47 MPa (5000 psi)
$\eta_{tot}$



SYSTEM B
34.47 MPa (5000 psi)
$\eta_{vol}$

SYSTEM B
34.47 MPa (5000 psi)
displacement fraction



SYSTEM B
34.47 MPa (5000 psi)
power loss

SYSTEM B
34.47 MPa (5000 psi)
total flow

1 [10³m³/s]   2   3   4



SYSTEM B
27.58 MPa (4000 psi)
$\eta_{tot}$

.8
.7
.7
.6
.5
.4

SYSTEM B
27.58 MPa (4000 psi)
$\eta_{vol}$



SYSTEM B
27.58 MPa (4000 psi)
displacement fraction

SYSTEM B
27.58 MPa (4000 psi)
power loss



SYSTEM B
27.58 MPa (4000 psi)
total flow

SYSTEM B
20.68 MPa  (3000 psi)
$\eta_{tot}$



SYSTEM B
20.68 MPa   (3000 psi)
$\eta_{vol}$

SYSTEM B
20.68 MPa (3000 psi)
displacement fraction



SYSTEM B
20.68 MPa (3000 psi)
power loss

100



SYSTEM B
20.68 MPa (3000 psi)
total flow

1 [10⁻³ m³/s]  2  3  4  5  6  7



SYSTEM B
13.79 MPa (2000 psi)
$\eta_{tot}$

.8
.7
.7
.6
.5

SYSTEM B
13.79 MPa (2000 psi)
$\eta_{vol}$



SYSTEM B
13.79 MPa (2000 psi)
displacement fraction

SYSTEM B
13.79 MPa (2000 psi)
power loss



SYSTEM B
13.79 MPa (2000 psi)
total flow

System B
6.895 MPa (1000 psi)
$\eta_{tot}$



System B
6.895 MPa (1000 psi)
$\eta_{vol}$

System B
6.895 MPa (1000 psi)
Displacement fraction



System B
6.895 MPa (1000 psi)
Power Loss (kNm/s)

SYSTEM A

34.47/13.79 MPa (5000/2000 psi)

$\eta$ tot

GEAR SHIFT

F [kN]



SYSTEM A

34.47/13.79 MPa (5000/2000 psi)

$\eta$ vol

GEAR SHIFT

v [m/s]

SYSTEM A
34.47/13.79 MPa (5000/2000 psi)

DISPLACEMENT FRACTION



SYSTEM A
34.47/13.79 MPa (5000/2000 psi)

POWER LOSS (kWm/s)

SYSTEM A
34.47/13.79 MPa (5000/2000 psi)

TOTAL FLOW  ( $10^{-2}$ m$^3$ / s)

GEAR SHIFT

.7
.6
.5
.4
.3
.2
.1

10.        20.    v [m/s]    30.



SYSTEM A
27.58/6.895 MPa (4000/1000 psi)

$\eta_{tot}$

.8

.7

.7

GEAR SHIFT

.6
.5

10.        20.    v [m/s]    30.

SYSTEM A
27.58/6.895 MPa (4000/1000 psi)

η vol

GEAR SHIFT



SYSTEM A
27.58/6.895 MPa (4000/1000 psi)

DISPLACEMENT FRACTION

GEAR SHIFT

110



SYSTEM A

27.58/6.895 MPa (4000/1000 psi)

POWER LOSS  (kNm/s)



SYSTEM A

27.58/6.895 MPa (4000/1000 psi)

TOTAL FLOW  ($10^{-2} m^3/s$)

SYSTEM A

24.13/3.447 MPa (3500/500 psi)

$\eta_{tot}$



SYSTEM A

24.13/3.447 MPa (3500/500 psi)

$\eta_{vol}$

112



SYSTEM A

24.13/3.447 MPa (3500/500 psi)

DISPLACEMENT FRACTION



SYSTEM A

24/3/3.447 MPa (3500/500 psi)

POWER LOSS (kHm/s)

SYSTEM A

24.13/3.447 MPa (3500/500 psi)

TOTAL FLOW ( 10⁻² m³ / s )